

NASA Contractor Report 181611

THE EFFECT OF STING INTERFERENCE AT LOW SPEEDS
ON THE DRAG COEFFICIENT OF AN ELLIPSOIDAL BODY
USING A MAGNETIC SUSPENSION AND BALANCE SYSTEM

A. W. Newcomb

(NASA-CR-181611) THE EFFECT OF STING INTERFERENCE AT LOW SPEEDS ON THE DRAG COEFFICIENT OF AN ELLIPSOIDAL BODY USING A MAGNETIC SUSPENSION AND BALANCE SYSTEM (Vigyan Research Associates) 79 p CSCL 01A G3/02 N88-20274
Unclas 0135286

VIGYAN RESEARCH ASSOCIATES, INC.
Hampton, Virginia

Contract NAS1-17919
February 1988



National Aeronautics and
Space Administration

Langley Research Center
Hampton, Virginia 23665

ABSTRACT

A Boltz body of revolution (finenessratio 7.5:1) was tested in the SUMSBS. The effects of sting interference on the drag coefficient of the model at zero angle of attack were noted as well as the effects on drag coefficient values of boundary layer trips. The drag coefficient values were compared with other sources and seemed to show agreement.

The pressure distribution over the rear of the model with no sting interference was investigated including the use of boundary layer trips.

CONTENTS

PAGE NO.

ABSTRACT	i
CONTENTS	iii
LIST OF FIGURES, TABLES AND APPENDICES	iv
SYMBOLS AND ABBREVIATION	v
1. INTRODUCTION	1
2. INITIAL DESIGN	2
2.1 Models	
2.2 Stings	
2.3 Optics	
2.4 Manometers	
2.5 Data analysis programs	
3. PRELIMINARY TESTING AND REDESIGN	10
4. CALIBRATIONS	12
4.1 Pressure calibration	
4.2 Force-current calibration	
5. TESTING	13
5.1 Drag investigation	
5.2 Pressure investigation	
6. RESULTS AND DISCUSSION	16
6.1 Comparison of sting free and sting based models Cd values	
6.2 Comparison of results with other sources	
6.3 The effects of tripping the boundary layer	
6.4 Sources of error	
7. CONCLUSIONS	22
8. RECOMMENDATIONS	23
8.1 Improvements to the system	
8.2 Suggestions for future investigations	
9. ACKNOWLEDGEMENTS	24
10. REFERENCES	25
FIGURES	26
TABLES	44
PRECEDING PAGE BLANK NOT FILMED	
APPENDICES	48

LIST OF FIGURES

1. Design drawing of Boltz body of revolution
2. Design of rear of Boltz body
3. Design of rear of Boltz body for use with the sting
4. Design of rear of Boltz body for pressure distribution measurements
5. Design of sting support strut
6. Changes needed to the top of the test section
7. Design of sting support sleeve, and dummy sting
8. Design of pressure take off sting
9. Design of perspex window for the bottom of the test section
10. Design of rod mount and mirror mounts
11. Dynamic pressure calibration
12. Axial force-current calibration
13. Drag coefficient vs Reynolds' number
14. Comparison of drag coefficients with other sources
15. Variation of C_p at the two rearmost tappings with Reynolds' number
16. Variation of C_p with axial position at Reynolds' number of $3.6 \cdot 10^5$
17. Variation of C_p with axial position at Reynolds' number of $8.8 \cdot 10^5$

LIST OF TABLES

1. Co-ordinates of surface of Boltz body of revolution
2. Measured values of C_p and Reynolds' number at the four static tappings
3. Example of output from program 4PROG1
4. Example of output from program 4PROG2

LIST OF APPENDICES

1. Calculation of pressure coefficients
2. Calculation of baseforce acting on the dummy sting model
3. Listing of 4PROG1 FOR
4. Listing of 4PROG2 FOR
5. Listing of 4MSBS3 MAC
6. Listing of 4MSBS DAT
7. Photographs of apparatus

LIST OF SYMBOLS

Characters

A	area
a	quadratic pressure distribution = $a + br + cr^2$
b	quadratic pressure distribution = $a + br + cr^2$
Cd	drag coefficient
Cp	pressure coefficient
c	quadratic pressure distribution = $a + br + cr^2$
H	total pressure
M	Mach number
P(r)	pressure as function of base cavity radius
p	pressure
q	dynamic pressure
R	maximum radius in base cavity
Re	Reynolds' number
r	radius
x	axial co-ordinate
y	radial co-ordinate

Subscripts

m	denotes 'model'
REF	denotes 'reference'
r	denotes 'reference'
oo	denotes 'free stream value'

Abbreviations

MSBS	Magnetic suspension and balance system
SUMSBS	Southampton University magnetic suspension and balance system

1. INTRODUCTION

The latest development of the Southampton University Magnetic Suspension and Balance System was the completion of a new low speed, octagonal section, wind tunnel in 1986.

A NASA Technical Note, ref. 1, gave drag coefficient values for a Boltz body of revolution which appeared to be very low. It was, therefore, decided to test a similar body in the SUMSBS low speed wind tunnel. With the body suspended magnetically drag data for the true model shape could be obtained, but by bringing up a dummy sting to the rear of the model it was hoped to simulate sting interference and check the seemingly low drag coefficients.

An investigation was also carried out into the pressure distribution over the rear of the model. As there was no supporting sting to interfere with the flow around the base of the model the resulting pressure distribution should be more accurate than would be obtained on a sting supported model.

2. INITIAL DESIGN

Several areas of design had to be considered for this project. The models and associated stings, the optical system, changes to the test section, and data analysis programs.

2.1 Models

The model used in this investigation was the one made for the honours project conducted by R. Knight, ref. 2. A set of body surface co-ordinates is given for the model in Table 1, and it is shown in Appendix 7. The model is comprised of two pieces. The major part being the hollow forebody extending to 79% chord, i.e. 79% of the total length, the complete model being 184.2mm long. The rear body acts as a plug allowing access to the magnets in the model. The maximum cross-sectional area, the reference area, is 0.00047 metres square.

Three rear bodies were made, one to accept the dummy sting, one to allow pressure plotting over the rear of the model, and one "true" shaped to allow testing of a sting free body.

2.1.1 The rear body designed for the dummy sting, Figure 3, was designed to have a cavity in it large enough for the model to be suspended without touching the dummy sting. NASA had tested a similarly shape sting supported model, ref. 1. Their model was 96 inches in length on a 4 inch diameter sting. Scaling this down to the length of the model in this investigation of 7.67mm. The cavity in the rear body was bored out to 8mm diameter. If testing showed the clearance to be too small the base would be increased until satisfactory. The design called for the hollow to be 6mm deep with an end face perpendicular to the sides, but a workshop error resulted in a "V" shaped end face.

2.1.2 The rear body designed to allow pressure readings to be taken over the rear of the model is shown in Figure 4 and in Appendix 7. The rear body was made like a true rear body, but a radial slot was machined out as shown. The slot was cut deep enough and wide enough to allow a small diameter hollow tube to run along the length of the rear body but beneath the surface. The slot was filled in with Araldite, holding the tube in position. The Araldite was then smoothed down flush with the surfaces of the model.

2.1.3 The tube was chosen as 20 gauge as this was thought to be the smallest diameter that would be easy to bend without causing collapse, and reasonably easy to drill into. The tube would emerge on the centre line as shown, allowing a rubber tube to be connected to it, connecting the model to a manometer.

2.1.4 Four holes were drilled into the tube at the positions shown in Figure 4. The holes were 0.3mm in diameter. Three of the holes would be sealed with plasticine at any one time so that pressures could be measured at one chordwise station. The plasticine was also used to smooth in any indentations in the Araldite.

2.1.5 The models were made from Aluminium as it is light, easy to machine and is magnetically stable. The magnetic core was made up of samarium-cobalt magnets as they are magnetically stable and would not require continual re-magnetisation as with some other materials. Care had to be taken when handling them as they are very brittle.

2.2 Stings

Two stings were necessary, one to represent a support sting, and the other to act as a pressure take off line. The major design considerations being enough stiffness to reduce vibration at the free end of the sting, as little blockage of the tunnel as possible, ease of use, and ease of fabrication.

2.2.1 The stings were designed to be supported on a strut which is shown in Figure 5 and is visible in Appendix 7. Rather than have the support strut fixed to the inside of the test section it was designed to fix to the outside of the test section causing less disruption to the air-flow. The strut would then pass through a slot cut into the test section. With the support strut in place the test section would be too large to fit through the axial electromagnets so the strut would have to be fixed in place once the test section was positioned in the MSBS. The only part of the test section that would take the support strut without having to partially dismantle the MSBS was the rear of the test section that protrudes from the MSBS. This dictated the length of the sting as it would have to reach forwards to where the model was suspended. The axial length of the support strut was chosen as 80mm and the width as 10mm in order to provide a stable support for the sting. The height of the strut

and the shape of the channel to accept the sting were chosen, once the sting diameter had been decided on, so that the sting could be positioned on the centre line of the test section.

2.2.2 To provide good stiffness the two stings were designed to fit into a common support sleeve which would be attached to the strut. The sleeve would reach forwards acting as an outer casing, the required sting could then be inserted into the end of the support sleeve and clamped in position. The inner diameter of the sleeve was determined by the outer diameter of the 'support' sting at $\frac{5}{16}$ inch. The outer diameter of the sleeve was chosen as 13mm to give a reasonable wall thickness. The sleeve design is shown in Figure 7 and in Appendix 7.

2.2.3 The design of the 'support' sting is shown in Figure 7 and Appendix 7. The required diameter of the sting was 7.67mm. Brass rod was available of diameter $\frac{5}{16}$ inch. This set the inner diameter of the support sleeve. As Figure 7 shows the 'support' sting was designed with a separate end piece. This had three pressure tappings drilled into it, each connected to a 20 gauge tube. This would allow model base pressures to be measured. Once the tubes had been soldered to the end piece the end piece was fixed to the sting. The first 65mm of the sting was then turned down to 0.3 inch or 7.62mm. The tubes were long enough to protrude from the open end of the sting, allowing rubber pipes to be connected, and the pressures taken off to a manometer. The length of the sting was set at 220mm. This was to allow a large range of movement of the front of the sting for changing the axial position of the model/sting combination.

2.2.4 The design of the pressure take off sting is shown in Figure 8 and Appendix 7. It was designed with a short length of 20 gauge tubing, to take the rubber pipe connected to the model, soldered into a larger tube to provide stiffness. A short length of tubing was soldered into the other end to enable a rubber pipe to take the pressure off to a manometer. The larger tube ran through, and was fixed to, a brass rod of $\frac{5}{16}$ inch diameter. The whole unit would then fit into the support sleeve and be clamped in place.

2.3 Optics

The standard set up for the axial position sensing system was to have a laser beam fanned out axially, illuminating a long thin detector.

The rear of the suspended model would then be in part of the laser beam casting a shadow on a portion of the detector. This system would not work in this investigation as the 'support' sting or pressure take off pipe would be in the way of the fanned out laser.

The two major alternatives were to have a similar system but using the front of the model, or a system with the laser fanning out across the test section.

The former would pose problems when trying to launch and retrieve the model. It was, therefore, decided to concentrate on the latter method.

2.3.1 There was only a small window in the bottom of the test section, so this was taken out and replaced by a perspex window of the same length, but greater width, enough to span the flat inner surface of the bottom of the test section. Its dimensions can be found in Figure 9.

2.3.2 It was wanted to illuminate the entire width of the bottom surface of the test section with the laser beam. The beam fanning glass rod could have been situated in several places but a position just before the first mirror was chosen as this would provide the most rigid mounting point and would be easier to align with the laser. The laser beam used, a 1mW helium-neon laser, provides a beam with a Gaussian intensity distribution. When the beam is fanned out the beam is less intense at its edges than near its centre. Also some intensity will be lost at the edges due to greater reflection losses from the two perspex windows. To increase the intensity at the edges and make the beam more uniform the beam was over expanded and only the central portion directed down through the test section. By looking at the action of several diameters of glass rod a glass rod with a diameter of 3mm was chosen to fan out the laser beam.

2.3.3 The laser beam would travel from the laser through the glass rod and then on to a mirror changing the beam direction so that it would run between the top of the test section and the upper electromagnets. It would then reach another mirror which would change the beam direction so that it passed through the test section onto the detector.

Two front reflecting mirrors, 25mm x 16mm, were available and were chosen. They were mounted on plastic card and the card was then stuck onto the mirror mounts as shown in Figure 10. The card allowed the mirrors to be removed from the mounts without damaging the mirrors.

The mirror mounts were designed to fit on the existing rod and rail system within the MSBS. The rods can be moved back and forth above the test section, allowing the laser beam to be reflected down through a different section of the test section.

2.3.4 The beam fanning glass rod was mounted on the rod mount shown in Figure 10. The mount was then attached to the existing rails in the MSBS.

2.3.5 Initially the existing detector was used, the only change made being to mount it transversely. See Section 3 for changes that eventually had to be made.

2.4 Manometers

When running the tunnel two pressures must always be known. Atmospheric pressure and the reference dynamic pressure in the tunnel. Atmospheric pressure was measured on a standard mercury barometer. In tests with the dummy sting the three base pressures must also be measured. This means four pressures have to be measured. The tunnel was known to operate with a maximum dynamic pressure of 3kPa. Using methylated spirit with a specific gravity of 0.83 3kPa is represented by a head of 0.37 metres. The resulting manometer height chosen was 0.8 metres which allowed the manometers to be used at higher pressures should this be possible in the future. The manometers were made by the Chemistry Department's glass blowing service, with a bore of 6mm.

2.4.1 Five such tubes were mounted on a board with a metric graph paper scale between the tubes and the board. The board was then mounted on the inlet to the tunnel. As the tubes are fairly fragile the board was arranged so that it could be removed easily for safer storage. The fifth tube allowed for any future need to measure five pressures.

2.5 Data Analysis Programs

2.5.1 Data Storage

When running the MSBS the user can store current and position data for future analysis. The MSBS runs at 400 Hz, the amount of information storeable is set by an array in 4MSBS3 FOR in this case 750 cycles, or $1\frac{7}{8}$ of a second worth of data. Looking at the currents data over a second it could be seen that the currents varied considerably. Just taking a small portion of data would not reliably represent the currents in the electromagnets. Data was, therefore, taken over one second at set intervals, 50 cycles total being read. This was arranged by using the data file 4MSBS DAT see Appendix 6. When the MSBS was running typing 1g caused 50 cycles to be stored, the data being taken over a one second period. Typing 2g could cause 100 cycles to be stored, the first fifty then a seconds break and then the next fifty.

2.5.2 On stopping the controlling program the data taken could be saved into a file of the user's choice for later analysis.

2.5.3 Program 1

An existing Fortran IV program was adapted, the new version 4 PROG 1 FOR being in Appendix 3. On running it would ask for the file name of the file in which the current data was stored, along with the room temperature and pressure in celsius and kPa respectively. It then asks the user how many blocks of data are to be read from the data file and whether the output is to the screen⁽⁵⁾ or the printer⁽⁶⁾. When running the MSBS typing 1g results in 50 cycles worth of data being stored. The data is read over a second as five blocks of ten cycles. Hence to read in 1g worth of current data the user must ask for five blocks to be read in, ten blocks for 2g, etc.

2.5.4 The program reads in the required number of blocks and calculates the average of the sum of the axial currents of each cycle, and also the standard deviation from that average. Using Chauvenet's criterion for error rejection any 'bad' cycles are rejected the new average currents and positions being calculated.

2.5.5 The program then asks for the date when the data was taken. The date to be inputted in a coded form. If the wind was off and the data

is the first set then the format is "START date". If the wind was off and the data is the last set then the format is "STOP date". If one of these is used the program asks if the user wishes to continue. If the data is not the first or last set then a different format must be used. If the dummy sting was present when the data was taken the format is "YS date", the program then goes on to ask for the three base pressures and the reference dynamic pressure in kPa, and then on to ask if the user wishes to continue. If the dummy sting was not present the format is "NO date", the program then asks only for the reference dynamic pressure, and then on to ask if the user wishes to carry on and analyse the next block(s).

2.5.6 Once all the data has been read in the averaged current data for each block along with average position data, pressures and temperature, and the date are saved in the file 4PROG1 STO which is used in the next program. The data can also be added to a master file 4CURR DAT with the averaged currents of all the runs to date stored in it.

2.5.7 The data is saved with the "START date" and "STOP date" being saved first. This means that when the file is read in the next program the current offsets can be changed before the wind on currents are read in.

2.5.8 Program 2

A listing of 4PROG2 FOR can be found in Appendix 4. After running 4PROG1 FOR this program is run. It reads in the contents of 4PROG1 STO one line at a time. If the data is a "START date" or "STOP date" then the respective current offset is reset and then next line is read in. If the date is not a "START date" or "STOP date" the program goes on to convert the axial currents to an axial force using a factor obtained from the current force calibration of section 4.2. The test section dynamic pressure is then calculated by multiplying the reference dynamic pressure by a value obtained from the pressure calibration in section 4.1. The density of the air and its kinematic viscosity are then calculated. It was assumed that the relative kinematic viscosity follows the relative absolute temperature to the power 0.8.

2.5.9 If the date signifies that the sting was not present the base force is set to zero, otherwise the baseforce is calculated. Knowing the three measured base pressures and the radii at which they were measured

the program assumes that the pressure varies as a quadratic function of radius. Calculating this function, see Appendix 2, the pressures acting on the base area are integrated up to give the acting baseforce.

2.5.10 The base force and the force provided by the axial magnets act in the same direction. The sum of the two is equal to the drag force on the model. Knowing the drag force, the dynamic pressure, and the reference area, $0.47 \cdot 10^{-3} \text{ m}^2$ the maximum cross sectional area, the drag coefficient is calculated. The test section free stream velocity, Mach number, and Reynolds' number, based on the length of the model, are then calculated.

2.5.11 The drag coefficient, Reynolds' number, free stream velocity, free stream Mach number, free stream dynamic pressure, total axial force (equal to the total drag force acting on the model), the baseforce, and the date are then written to the output file 4PROG2 STO.

2.5.12 The program then returns to read in the next line of data from 4PROG1 STO. If the line read in is the "END FILE" line the program asks if the user wants the data (Cd etc.) to be written to the master file 4CDRAG DAT. The program then saves the necessary files and then stops.

3. PRELIMINARY TESTING AND REDESIGN

3.1 As stated in Section 2.3.5 the axial position detector^t was initially mounted transversely. A red 'Cokin' filter was used to cut out as much ambient light as possible and also to protect the detector.

3.1.1 The model was suspended in the MSBS. It was found that the model oscillated axially about $\pm 5\text{mm}$ from an initial position. With the particular shape of the rear of the body being tested, i.e. a low curvature until near the end of the model, an axial movement only produces a small change in the shadow size and hence change in the output of the detector. With the model out of the MSBS the output of the detector fluctuated, due to variations in the intensity of the laser beam with time. This could be regarded as noise, and any change in output due to the model moving as the signal wanted. The axial oscillation would be reduced by increasing the signal to noise ratio.

3.1.2 This was initially performed by blanking off parts of the detector which previously would have always been illuminated regardless of the model's axial position. The oscillation was greatly reduced, but at times when the laser was fluctuating badly was still too high.

3.1.3 Several options were open; use a more consistent laser, position the laser at the front of the model with an axially fanned laser beam, use a digital sensor which would not interpret the slight changes in intensity as a position change, or use another detector to provide a reference signal indicating any changes in the intensity of the laser beam.

3.1.4 The first option was not possible. The second was discarded for the reasons given in Section 2.3. The third would pose a problem as the existing digital sensors are only about one inch in length and would have either required a collimated laser beam, or would have only been able to pick up the laser/shadow boundary on one side of the model if the beam was diverging as it had been set up to do. Only picking up the one boundary would pose problems as any yaw of the model would be interpreted as a large axial position change, if two boundaries were used this effect would nearly cancel out. The fourth option of using a reference sensor appeared to be the most likely solution given the time available.

3.1.5 A small, 6mm x 6mm photodetector was fixed in the same housing as the main detector. The reference detector was connected to an amplifier and analogue to digital converter using the "roll" channel which would have been unused in this investigation. The voltage from the reference sensor was present on channel one, and the voltage from the main detector on channel zero.

3.1.6 An existing Fortran IV program was modified to repeatedly read in both voltages and display them along with the changes from the previous values. The changes did not keep in step. The program was altered to display the changes from the first values read in. This gave much better results with the changes keeping in step for large fluctuations from the original values. For smaller changes of the reference detector the results were not so good. A threshold was built in so that only changes greater than a set value would result in a change being made to the value obtained from the main detector. The next step was to incorporate a MACRO version of the program into the control program, 4MSBS3 MAC, used to control the MSBS.

3.1.7 The final version of 4MSBS3 MAC is in Appendix 5. When the program is run the threshold value and scaling value are set at zero. These values could be altered while the program is running by typing in the new value along with a letter signifying the parameter to be changed, and then typing "1?" which initiates the changes. The reference outputs of the main sensor (setting the model's axial position) and of the reference sensor can be changed by the same method. The scaling factor used in the program has to be inputted as an integer. To allow a factor between one and two (which appeared to give the best results) the required factor is inputted in thousands i.e. 1500 for 1.5. For example to set a factor of 1.75, a threshold of 3, to move the model to a position such that the main sensor output is 2550 and to reset the reference sensor reference value to the instantaneous ready type 1750F 3T 2550M 1S 1?.

4. CALIBRATIONS

Two calibrations were necessary. One to relate the reference dynamic pressure to the dynamic pressure in the test section, and the other to relate the applied axial current to the acting drag force.

4.1 Pressure Calibration

The reference dynamic pressure was measured by a pitot tube and a static pressure tapping just aft of the contraction. The total pressure of the air flow was assumed constant along the tunnel. A static pressure tapping already existed in the test section. Two manometers were used to show the true dynamic pressure and the reference dynamic pressure. Also the difference between the two static pressures could be calculated. A plot of the two dynamic pressures is given in Figure 11. The relationship $q_{\text{TRUE}} = q_{\text{REF}} \cdot 1.017$ can be determined from the plot.

4.2 Force-Current Calibration

A static force-current calibration was used. An axial force was applied to the model, the resulting currents recorded and a plot of the results drawn up, see Figure 12. The force was applied by fixing one end of a length of cotton to the rear of the model, the other running over a pulley to a pan with weights on it. The plot has a gradient of 0.044 Newtons per amp, where the current is the sum of the axial currents.

5. TESTING

The testing was carried out in two blocks. Firstly the drag data was taken with and without the dummy sting, with and without boundary layer trips, and secondly an investigation into the pressures over the rear of the model with and without boundary layer trips was undertaken.

5.1 Drag Investigation

The model was suspended and moved into the position it occupied in the force-current calibration with the commands 280-m 300y 40z 2550M 1S 2T 1?. Any roll was taken out by holding the model so that it stopped oscillating and by releasing it carefully. The tunnel intake was then wheeled up to the test section, aligned using the aligning dowels and clamped to the test section. If the model was oscillating axially the oscillation was reduced as much as possible by inputting a series of scaling factors and then using what appeared to be the best one, e.g. 400F 1?.

5.1.1 Current data was recorded with the wind off. The wind was then turned on with the tunnel speed control set to either 3½V or 6V (the maximum is 10 Volts) to avoid low speed resonances in the fan unit. The required speed was then set and the flow allowed to stabilise for around a minute. Current data was taken and the necessary pressures noted down. Once all the wind on data had been taken the tunnel control was set to either 3½V or 6V the tunnel allowed to slow down, and then the fan unit switched off. Once the fan had stopped spinning and there was no, or negligible, flow through the tunnel a set of wind off data was taken.

5.1.2 The tunnel intake was removed from the front of the test section, and the model removed from suspension. The escape character was then pressed and the data saved into a file. The electromagnets were then switched off.

5.1.3 It had been planned that the sting should reach into the base cavity. In practice it was found that this was easy to do but that the model kept touching the sides of the sting due to "sloppiness" in the control system. It was, therefore, decided to suspend the model just

in front of the sting rather than to increase the diameter of the cavity. The change in model position had no noticeable effect on the base pressures so it was felt to be valid. Also the change in position meant that the integrators could be used to improve the position holding of the model.

5.1.4 The data was then analysed using the programs 4PROG1 FOR and 4PROG2 FOR with the calculated drag coefficients etc appearing in the file 4PROG2 STO.

5.1.5 Data was taken for several conditions. The sting-less model was tested with no boundary layer tip, and boundary layer tips at 40%, 60%, 75% and 85% of the chord of the model. The model with the dummy sting was tested without a boundary layer tip, and with a trip at 85% of the model's chord. The trips were made from two strands of copper wire twisted together and then soldered in a loop. The resulting trips were 0.012 inches in diameter. If necessary they were stuck to the model with a 'super glue'.

5.2 Pressure Investigation

The rear body with the pressure take off 'tube' had four static holes drilled through the araldite into the pressure tube. For testing three holes were smoothed over with plasticene so that only one hole was open.

5.2.1 The pressure take off sting, see Section 2.2.4, had connected at its rear end around four feet of small bore rubber tubing. The other end of the tubing passed through the support sleeve of the sting, out through the top of the test section, and was connected via an adapter to a larger bore pipe. The larger bore pipe was connected to one side of one of the manometer tubes, the other side being connected to the reference static pressure.

5.2.2 To launch the model required two people. The sting would be unclamped from the support sleeve and pulled forwards to the front of the test section. It was then connected to the model via a short length of tubing. The tubing connected to the other end of the sting was then pulled so that the sting and the model moved down the tunnel. The model was supported on a makeshift stand inside the test section while the sting was clamped into the support sleeve. Care had to be taken to

ensure that when the model was moved forwards to the limit of the short tubing it remained illuminated by the laser beam. Holding the model in one hand the stand was removed from the test section. Making sure that the hand holding the front of the model was not in the way of any light beams and that the model was central in the test section the controlling program was started by the other person, and the electromagnets switched on. If the MSBS did not pick up the model successfully the magnets were switched off. They were then switched on again. With practice the model launched first time.

5.2.3 The tunnel intake was then fitted, as in Section 5.1 and the tunnel turned on at $3\frac{1}{2}$ V or 6V. The required speed was set, the flow allowed to stabilise and the reference dynamic pressure and the difference between the pressure from the open static tapping on the model and the reference static pressure noted. The tunnel speed was then changed and the new pressures noted. Once the required data had been taken the tunnel was slowed down and then switched off. The tunnel intake was then removed. One person would hold the front of the model taking care not to interrupt any of the light beams. The other person would then switch off the electromagnets and stopping the controlling program. The stand was then used to support the model.

5.2.4 To make an alteration to the model, such as to put on a boundary layer trip, or open up a different static tapping, the sting was unclamped from its support sleeve and pulled forwards along with the model to the front of the test section. The model could then be disconnected from the sting and any alterations made.

5.2.5 Each of the four static tappings was used at the six speed settings used in the drag investigation with no boundary layer trip. and with boundary layer trips at 75% and 85% of the model's chord. The testing order was to seal three tappings, test with no trip at all the speed settings, then with the trip at 75% chord, and finally with the trip at 85% chord. The next tapping was then opened up, the previous one being sealed.

5.2.6 The pressure coefficients were calculated using the method in Appendix 1, the results being shown in Figures 15, 16 and 17 and Table 2.

6. RESULTS AND DISCUSSION

The investigation was carried out in two parts. The drag investigation was carried out first, and then the pressure distribution investigation. The results, however, have to be viewed as a whole with the drag results directly related to the pressure distributions.

6.1 Comparison of Sting Free and Sting Based Models' Cd Values

Figure 13 shows the variation of drag coefficient with Reynolds number. It can be seen that the Cd values for the model without a sting and with no artificial boundary layer trip are higher than the values for the model with a sting and without a trip. On the model without a sting the flow separates near the base due to the strongly adverse pressure gradient around the base, and a wake is formed. With the sting in position the rear body-sting shape is not curved so sharply, the pressure gradient is still adverse but much less so, and the flow is able to follow the shape of the rear body-sting. Separation may occur due to the radial distance between the end of the body and the sting, but it would be less severe than on the sting free model. As the flow around the base is more favourable the pressure drag is lower for the rear body-sting combination, and hence the drag coefficient is reduced.

6.1.1 The general trend of the trip-less models is that the Cd values fall as the Reynolds' number increases. This can be explained by the relative thinning of the boundary layer with increasing Reynolds' number. The tests were carried out over a low Mach number range (Max. 0.21) and over a low Reynolds' number range (Max. $8.7 \cdot 10^5$), the fall in Cd values was therefore expected. The fall is more consistent for the model with the sting than without the sting.

6.1.2 A possible reason for this could be that the separation of the boundary layer from the sting free model is unsteady, with nothing to fix the separation. Or the variation could be due to errors in the testing procedure. The tests on the sting free model were the first tests, and the testing procedure was subsequently improved. As described in Section 2.5.1 current data was taken in small batches over a second in an effort to obtain a better average of the currents. However, this system was not used initially. The currents for the sting free model with no boundary layer trip being taken continuously over an eighth of

a second, and hence more likely to pick up temporary fluctuations in the axial currents. This would follow through to the drag data.

6.2 Comparison of Results with other Sources

Figure 14 shows a comparison of the two trip free models' drag results with those obtained in references 1 and 3. It must be born in mind that the results obtained in this report are not corrected for wind tunnel interference effects, whereas the values from references 1 and 3 are. References 5 and 6 were consulted but did not give a useable method for a closed regular octagonal test section with a body of large chord relative to the test section height. Opposing flats in the test section are seven inches apart. The expected correction to the Cd values would be a decrease in the region of one to two percent.

6.2.1 Looking at the two solid line plots shows the results for sting based models. The results from ref. 1 are over a Reynolds' number range an order higher than the range attainable in the SUMSBS wind tunnel. They were taken at a constant Mach number of 0.1. The plot shows that as the Reynolds' number increases from $5 \cdot 10^6$ the Cd values increase. The lower Reynolds' number points show the curve to be levelling off. The Cd values obtained in the SUMSBS wind tunnel fall with increasing Reynolds' number. The two sets look as if they may join up. It would be interesting to take some data in the range $1 \cdot 10^6 < Re < 4 \cdot 10^6$ to see if the sets can be linked. The Cd values in ref. 1 are given as based on wetted area. They are shown in Figure 14 as being based on maximum frontal area, as are all the other Cd values.

6.2.2 The broken lines show the sting free models, from this investigation and from ref. 3 for an ellipsoid of fineness ratio 8:1. Both sets fall with Reynolds' number. The ellipsoid has a lower drag coefficient than the Boltz body used in this investigation, by around ten percent. Reference 3 suggests that as the ellipsoid's fineness ratio decreases the Cd value should fall, with the optimum ratio being 4;1. The Boltz body used has a fineness ratio of 7.5:1, the difference in shape must therefore account for the higher drag, and it suggests that for a given fineness ratio the Boltz body has over ten percent higher drag. Correcting the Boltz body for wind tunnel interference would only be expected to reduce the Cd values by around one to two percent.

6.3 The Effects of Tripping the Boundary Layer

Referring to Figure 15 the effect of using the boundary layer trips can clearly be seen. The trip alters the C_d value by several means. There is a change in C_d due to the drag of the wire itself, although this should be small relative to the total drag of the model. If the boundary layer is laminar when it reaches the trip it separates, to reattach further downstream as a turbulent boundary layer. The turbulent boundary layer produces a higher skin friction than a laminar boundary layer so the C_d will rise. However, the turbulent boundary layer is more energetic and is more able to withstand an adverse pressure gradient and the separation occurs further downstream. This results in a smaller wake and more pressure recovery over the base of the model, and the C_d falls. The total change in C_d depends on the position of the trip, too far forward and the skin friction outweighs the pressure recovery and the C_d value rises.

6.3.1 With the trip at 40% chord on the sting free model the C_d values increase dramatically over the no trip model. Initially the C_d rises to a peak and then falls off as Reynolds' number increases. This could be due to the pressure recovery over the base only being large enough to outweigh the increase in skin friction at higher Reynolds' numbers.

6.3.2 With the trip at 60% chord the behaviour is as for the trip at 40%, but not so great.

6.3.3 With the trip at 75% chord on the sting free model the C_d values are lower than the values for the no trip model. The trip is now acting beneficially, the pressure recovery outweighing the increase in skin friction aft of the trip. The C_d values fall with increasing Reynolds' number, but with an extra low C_d at a Reynolds' number of $7.2 \cdot 10^5$.

6.3.4 With the trip at 86% chord on the sting free model the same thing happens at a Reynolds' number of $7.2 \cdot 10^5$. The extra low value is not such a large variation from the other points as for the 75% trip plot.

6.3.5 From Figure 15 it can be seen that at the rearmost pressure tapping, at 97% chord, the C_p values drop slightly (become less positive) at a Reynolds' number of around $7.2 \cdot 10^5$. This would imply that the normal force at this position was decreasing, i.e. that the drag should increase. The C_p values for the tapping at 91% chord do not show a major change at

this Reynolds' number. These results are anomalous with the dip in Cd values at this Reynolds' number. This suggests that the dip in Cd values is due to changes in the pressure distribution over parts of the model that were not investigated, i.e. aft of 97% chord. Another possibility is discussed in Section 6.4.4.

6.3.6 The plot for the sting based model with a trip at 86% chord also shows strange behaviour at a Reynolds' number of $7.2 \cdot 10^5$, but in this case it is an increase in Cd value. There is no Cp information available to explain this.

6.3.7 The plot for the sting free model with a trip at 86% chord shows that at low Reynolds' numbers the Cd value is higher than the no trip values. As the Reynolds' number increases the Cd values drop below the no trip values. This low Reynolds' number behaviour does not occur with the trip at 75% chord, which has Cd values slightly lower than the no trip values, but it does occur with the sting based model with a trip at 86% chord.

6.3.8 From Figure 16 it can be seen that at the lowest Reynolds' number of $3.6 \cdot 10^5$ the Cp values with the trip at 75% chord only differ appreciably from the no trip values over the last nine percent of the chord, or maybe less if a different line is drawn through the points. As the axial position increases the Cp values become less negative until at 93% chord they become positive values, i.e. the pressures reduce the drag relative to the no trip model. The difference between the Cp at the 97% chord tapping is large, 0.3 with the trip as against -0.5 without the trip. With the trip at 86% chord there is a major change in Cp behaviour with axial position. The overall trend is still for the Cp values to become less negative with axial position, but until 94% chord, or more, the Cp values are more negative than the values for the no trip model. It seems therefore that the more negative Cp values, 86% chord trip relative to no trip, from 80% chord to 94% outweighs the less negative values over the last 6% of the chord and the Cd is actually increased relative to the no trip model.

6.3.9 With the trip at 75% chord the boundary layer reattaches^e after the trip, but with the trip at 86% and the model curvature much higher it may be that the boundary layer does not reattach.

6.3.10 As the flow is subsonic pressure information can be transmitted upstream and the separation could affect axial positions upstream of the trip.

6.3.11 The C_p values for the trip at 86% chord cannot be explained by a leak in the pipes carrying the pressure to the manometer as the C_p values for the Reynolds' number of $8.8 \cdot 10^5$ do not show any unusual behaviour, Figure 17, the two sets of data being taken at the same time, see Section 5.2.5.

6.3.12 Figure 17 shows the pressure variation over the rear of the model at a Reynolds' number of $8.8 \cdot 10^5$. The plot for the model with no trip shows the same trend as at the lower Reynolds' number, but the C_p values at 97% chord is less negative and therefore results in less drag. The plot for the trip at 86% chord shows the C_p values becoming less negative and finally positive reaching a C_p of +0.08 at 97% chord, accounting for the decrease in C_d over the no trip C_d value. With the trip at 75% chord pressure recovery occurs aft of 91% chord, but between 81% and 91% chord the C_p values are more negative than the no trip values.

6.3.13 Figure 13 shows that at the higher Reynolds' number the trip at 86% chord on the sting based model results in lower C_d values than the no trip sting based model. Possible reasons could be due to a limited pressure recovery over the remainder of the model's rear surface, or that the change in flow between the model and the sting is accomplished more easily and clearly with less disruption being transmitted upstream.

6.4 Sources of Error

The model used was representative of the Boltz body as defined in Table 1. However the model was not well made, deviating from the given co-ordinates. The model used in ref. 1 on the other hand was of extremely high quality. Also the construction of the model with a main forebody and a smaller rear body meant that the two sections had to be joined together. The joint between the two was not perfectly flush. It was feared that the joint may initiate transition, but this did not appear to be the case. The joint was at 79% chord. Figure 13 shows that with a trip at 75% chord there is a large drop in C_d values over the 'no trip' values. If transition was occurring at the joint the trip at 75% chord

would produce higher Cd values than the 'no trip' values due to the extra skin friction and wire drag. Therefore it seems that the joint does not initiate transition.

6.4.1 By looking at the currents in the axial electromagnets with the model in suspension and the wind off it could be seen that the axial currents varied by around $\pm 20\%$ from a mean value. This variation also incorporated the variation due to the axial position ~~SENSING~~ system picking up some of the fluctuations in intensity of the laser beam. This variation in axial current follows through directly into the Cd values. It is expected that the residual variation in axial currents would stay the same as the current increased, so the percentage change would drop. This appeared to happen with the scatter in Cd values being higher at lower Reynolds' number.

6.4.2 Each point on Figure 13 is the average of fifteen values. Each of the fifteen values is made up from fifty data points taken in five batches of ten data points. In this way it was hoped that the average value would be representative of the true value. With the average being taken of the fifteen values if one of those values was increased by twenty percent the average would change by less than two percent.

6.4.3 The pressure investigation was carried out with a small diameter (20 gauge) tube protruding from the rear of the model, see Section 2.1.2. The rearmost pressure tapping was at 97% chord and it is felt that the pressures measured there would only be slightly affected by the tube.

6.4.4 The flow through the test section has not yet been surveyed. The flow seemed steady, but it is interesting to note that the flow was not as steady with the fan voltage at 8V which corresponds to a Reynolds' number of $7.2 \cdot 10^5$. This was the Reynolds' number at which the kinks appeared in the drag coefficient vs Reynolds' number plot see Figure 13 and Section 6.3.3 to 6.3.6 inclusive. The models were positioned in the centre of the test section.

7. CONCLUSIONS

The drag coefficient values obtained suggest that the seemingly low values attained in ref. 1 could be correct, and due to the change in base flow due to sting interference, and to Reynolds' number effects.

The general trend of drag coefficient with Reynolds' number, over the Reynolds' number range attainable in the SUMSBS low speed wind tunnel, is that the drag coefficient values fall with increasing Reynolds' number.

The drag coefficient values for sting free model are generally 15% higher than the values for the sting based model. This shows the importance of allowing for sting interference effects, and the benefits of an MSBS.

The use of boundary layer trips has a large effect on drag coefficient values, and hence when testing obtaining a similar transition point to full scale is crucial.

The MSBS allowed pressure plotting over most of the rear of the model. The results showed the expected trends, although data from more axial position would have been useful. The method worked easily, but there was room for improvement.

8. RECOMMENDATIONS

8.1 The present MSBS and wind tunnel could be improved by:

1. The further development and use of a digital axial position sensing system which would not be affected by the small fluctuations in the intensity of the lower beam.
2. Combining the fan speed control and on/off switch in one unit next to the wind tunnel.
3. The control system program be optimised to provide better model control.
4. The elimination of the low speed fan unit resonances.
5. Fitting a trap door in the diffuser allowing easy retrieval of any model flyaways. The model was only lost twice, both when the fan was turned straight from full on to off and even then the model stayed in the test section.
6. The fitting of a seal between the test section and the air intake.

8.2 Suggestions for further investigations are:

1. To carry out an accurate velocity traverse of the test section.
2. To carry out sting interference tests with the model at various angles of attack.
3. To extend the C_p investigation further to the rear of the model, and also to check the values obtained in this report.
4. The possible development of a solid-state on-board pressure sensor able to transmit data to a receiver without a physical link. This would allow testing right up to the trailing edge of the model, with no interference.

9. ACKNOWLEDGEMENTS

It is an impossible task to acknowledge all the people who have contributed to this report. However, I would like to express my sincere thanks to all those people, and in particular:

Jon Eskins for his continuous help and encouragement in all areas of this work, as well as Mark Lewis, Graeme Neal, and David Parker for their comments and patience when I needed to run the MSBS.

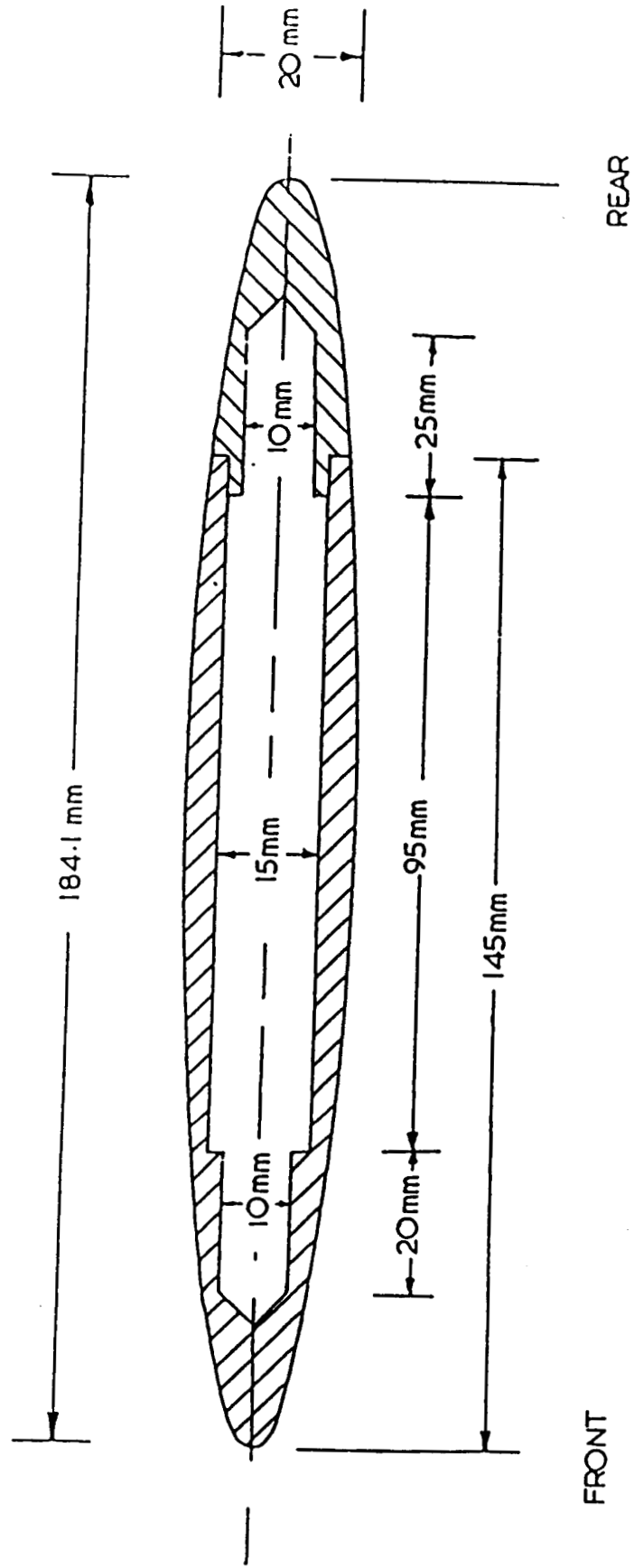
The various Departmental workshops for constructing models, apparatus, changing the test section windows, and the forming of the glass manometer tubes.

Finally, my supervisor, Dr. M. J. Goodyer for his support, advice and guiding comments.

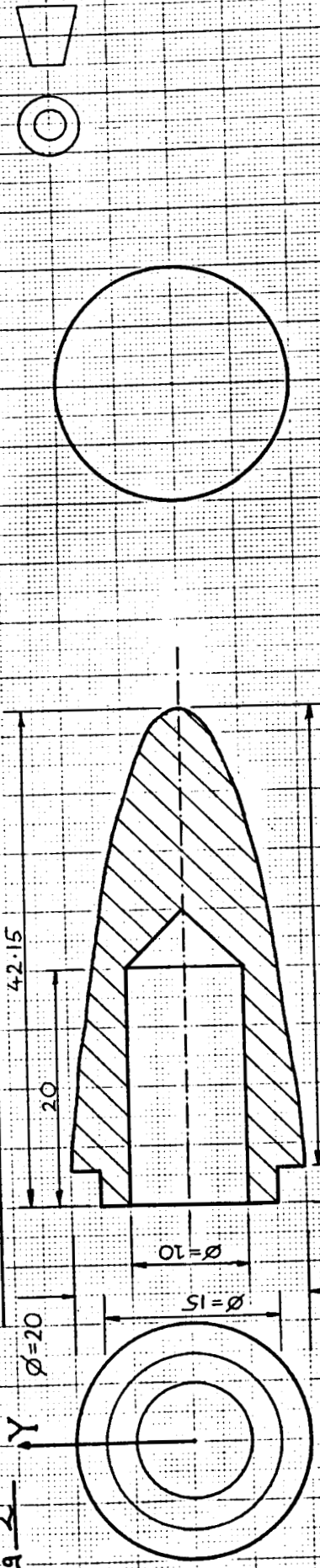
10. REFERENCES

1. Boltz, F.W., Kenyon, G.C., Allen, C.Q.: The boundary layer transition characteristics of two bodies of revolution, a flat plate, and an unswept wing in a low turbulence wind tunnel. NASA TN-D-309, April, 1960.
2. Knight, R.S.: The completion of the Department's magnetic suspension and balance wind tunnel and a preliminary drag study on a blunt body of revolution. University of Southampton, Department of Aeronautics and Astronautics, B.S.C. project May, 1986.
3. Judd, M, Viajinac, M., Covert, E.E.: Sting-free drag measurements on ellipsoidal cylinders at transition Reynolds' numbers. J. Fluid Mech. (1971), Vol. 48, part 2, pp 353-364.
4. Britcher, C.P.: The Southampton University Magnetic Suspension and Balance System - A Partial User Guide. AASU Memo. 83/8.
5. Pankhurst, R.C., Holder, D.W.: Wind-tunnel technique. Ptman 1952.
6. Garner, H.C. Rogers, E.W.E., Acum, W.E.A., Maskell, E.C.: Subsonic Wind Tunnel Wall Corrections. AGARDograph 109, October, 1966.
7. Hoerner, S.F.: Fluid-dynamic drag. 3rd ed. Bricktown N.W. 1965.

Fig 1 Design of Boltz body



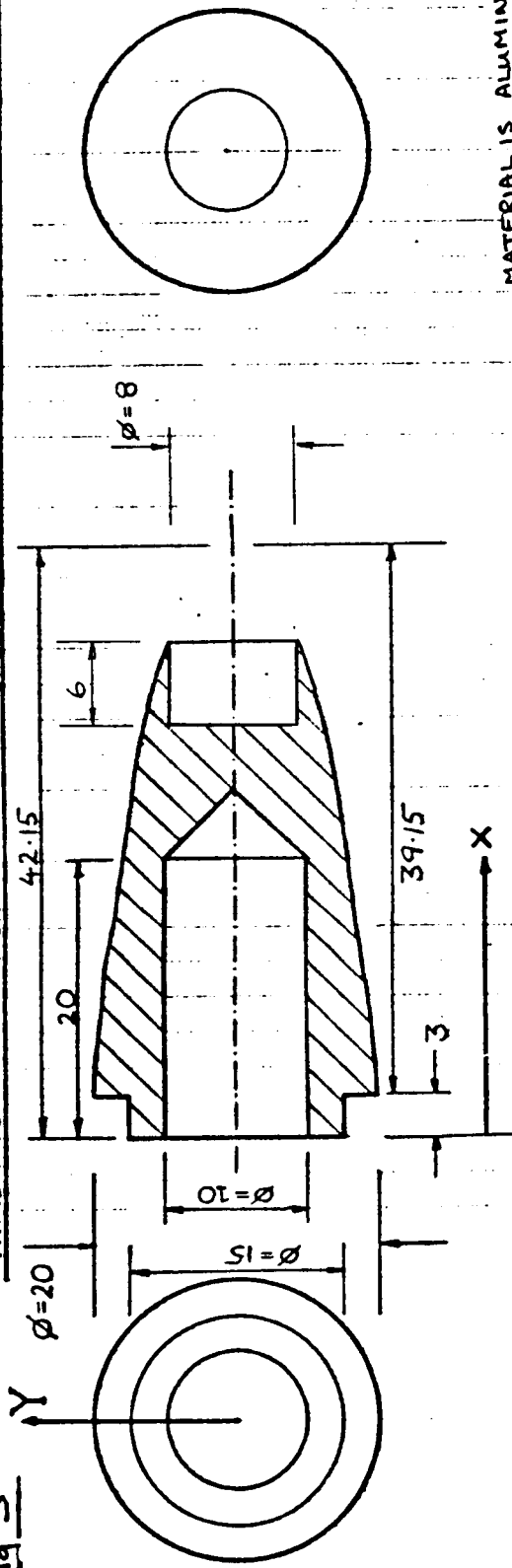
THIRD ANGLE PROJECTION OF REAR OF BOLT BODY WITH COORDINATES, DIMENSIONS IN MM



MATERIAL IS ALUMINIUM

X (mm)	Y (mm)	X (mm)	Y (mm)	X (mm)	Y (mm)	X (mm)	Y (mm)
0	7.5	26.806	6.789	41.078	1.871	42.091	0.448
2.9	7.5	28.341	6.470	41.231	1.733	42.121	0.318
3.0	10.0	29.875	6.128	41.385	1.582	42.137	0.224
5.322	9.826	31.410	5.758	41.538	1.416	42.152	2.7691 × 10 ⁻⁸
8.391	9.505	32.944	5.354	41.692	1.226		
11.460	9.155	34.480	4.909	41.845	1.002		
14.529	8.772	36.014	4.410	41.922	0.869		
17.598	8.351	37.548	3.835	41.999	0.709		
20.668	7.886	39.083	3.144	42.029	0.634		
23.739	7.369	40.624	2.233	42.060	0.549		

Fig 3 THIRD ANGLE PROJECTION OF REAR OF BOLT BODY WITH COORDINATES, DIMENSIONS IN MM



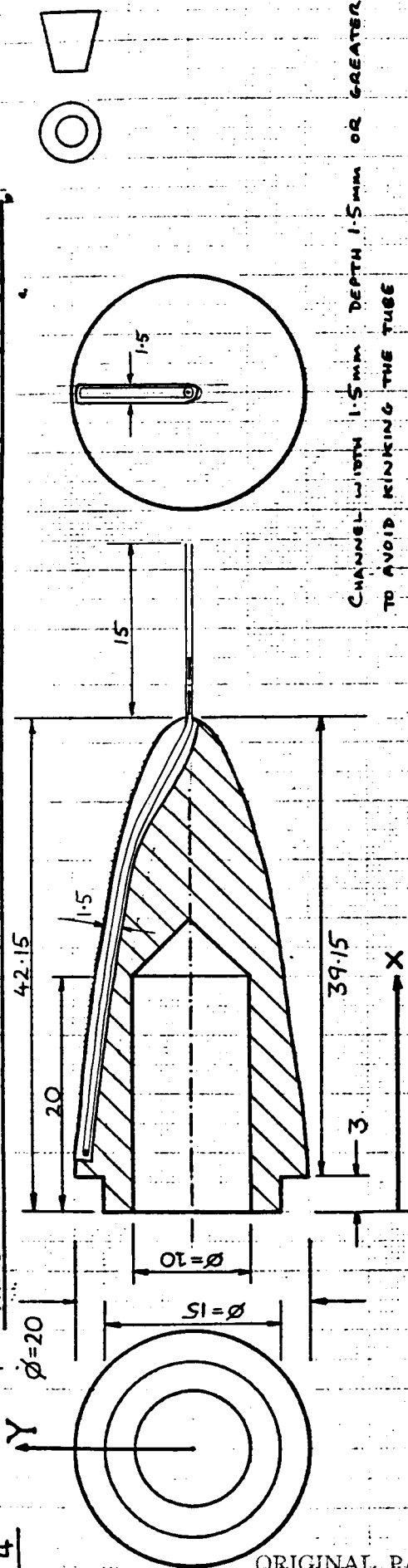
MATERIAL IS ALUMINIUM

COORDINATES BEFORE BORING OUT

X (mm)	Y (mm)	X (mm)	Y (mm)	X (mm)	Y (mm)	X (mm)	Y (mm)
0	7.5	26.806	6.789	41.078	1.871	42.091	0.448
2.9	7.5	28.341	6.470	41.231	1.733	42.121	0.318
3.0	10.0	29.875	6.128	41.385	1.582	42.137	0.224
5.322	9.826	31.410	5.758	41.538	1.416	42.152	2.7691 × 10 ⁻⁸
8.391	9.505	32.944	5.354	41.692	1.226		
11.460	9.155	34.480	4.909	41.845	1.002		
14.529	8.772	36.014	4.410	41.945	0.869		
17.598	8.351	37.548	3.935	41.922	0.709		
20.668	7.886	39.083	3.144	41.949	0.634		
23.739	7.369	40.924	2.233	42.029	0.549		
				42.060			

Fig 4

THIRD ANGLE PROJECTION OF REAR OF BOLT BODY WITH COORDINATES, DIMENSIONS IN MM



CHANNEL WIDTH 1.5 MM DEPTH 1.5 MM OR GREATER
TO AVOID KINKING THE TUBE

TUBE IS 20 GAUGE OPEN AT PROJECTING END, CLOSED
AT OTHER END

CHANNEL TO BE FILLED IN WITH AGALBITE THEN RUBBED SMOOTH
POSITION OF STATIC HOLES AT X = 5, 12, 22, 33 MM

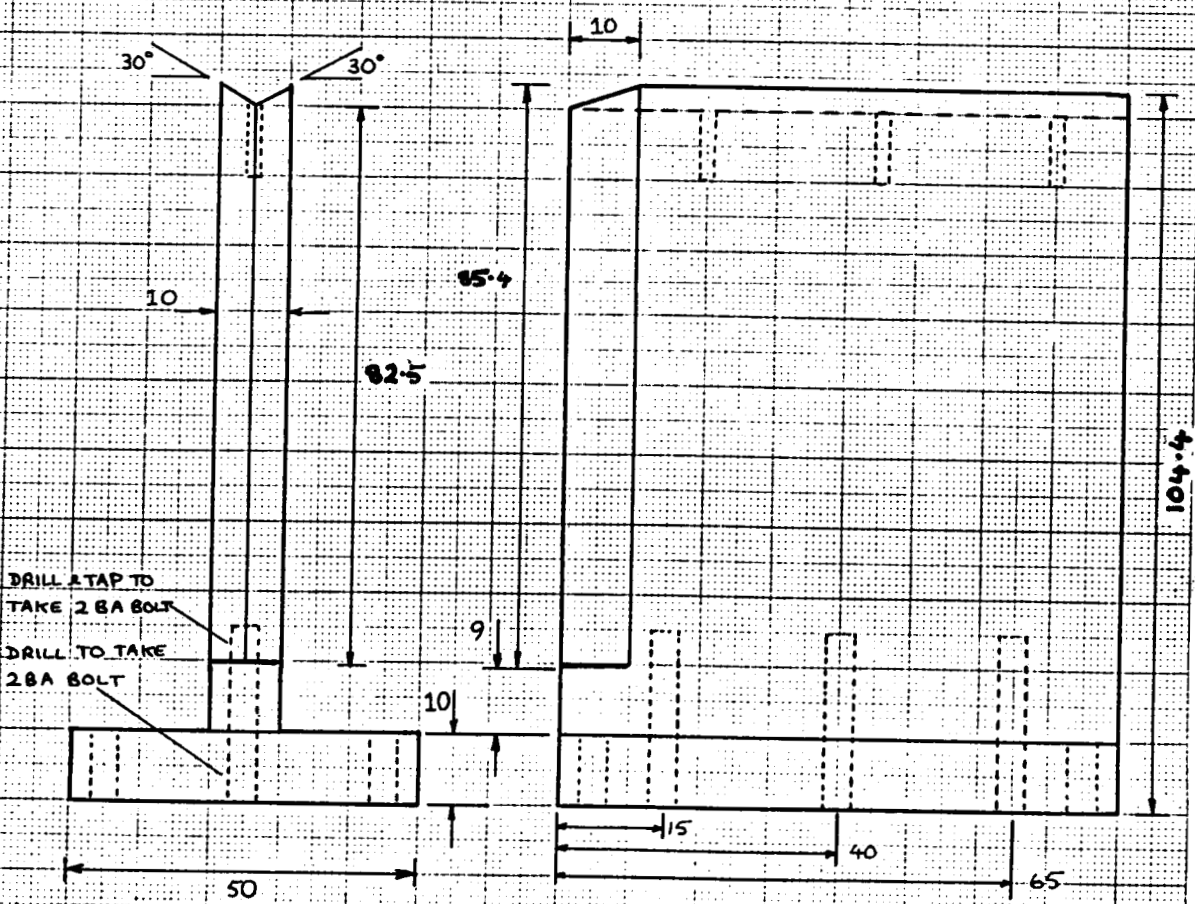
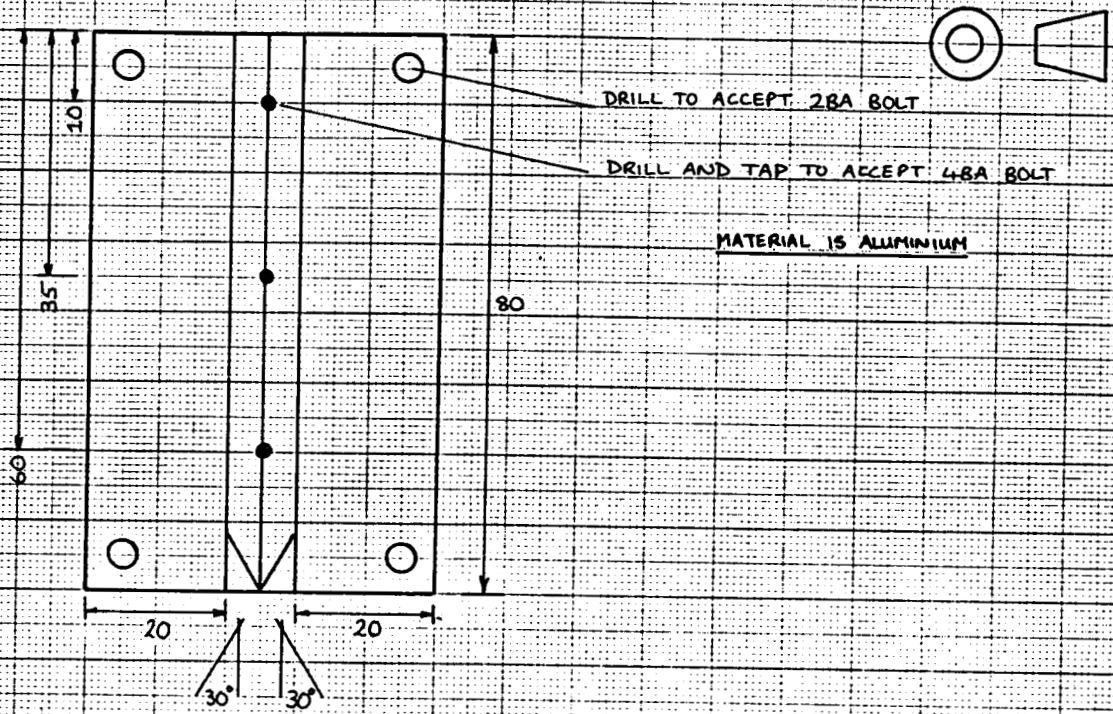
SURFACE COORDINATES

X (mm)	Y (mm)	X (mm)	Y (mm)	X (mm)	Y (mm)
0	7.5	26.806	6.789	41.078	1.871
2.9	7.5	28.341	6.470	41.231	1.733
3.0	10.0	29.875	6.128	41.385	1.582
5.322	9.826	31.410	5.758	41.538	1.416
8.391	9.505	32.944	5.354	41.692	1.226
11.460	9.155	34.480	4.909	41.845	1.002
14.529	8.772	36.014	4.410	41.922	0.869
17.598	8.351	37.548	3.935	41.999	0.709
20.668	7.886	39.083	3.144	42.029	0.634
23.739	7.369	40.624	2.233	42.060	0.549

X (mm)	Y (mm)
42.091	0.448
42.121	0.318
42.137	0.224
42.152	2.7691 x 10 ⁻⁸

Fig 5

THIRD ANGLE PROJECTION OF STING SUPPORT, DIMENSIONS IN MM

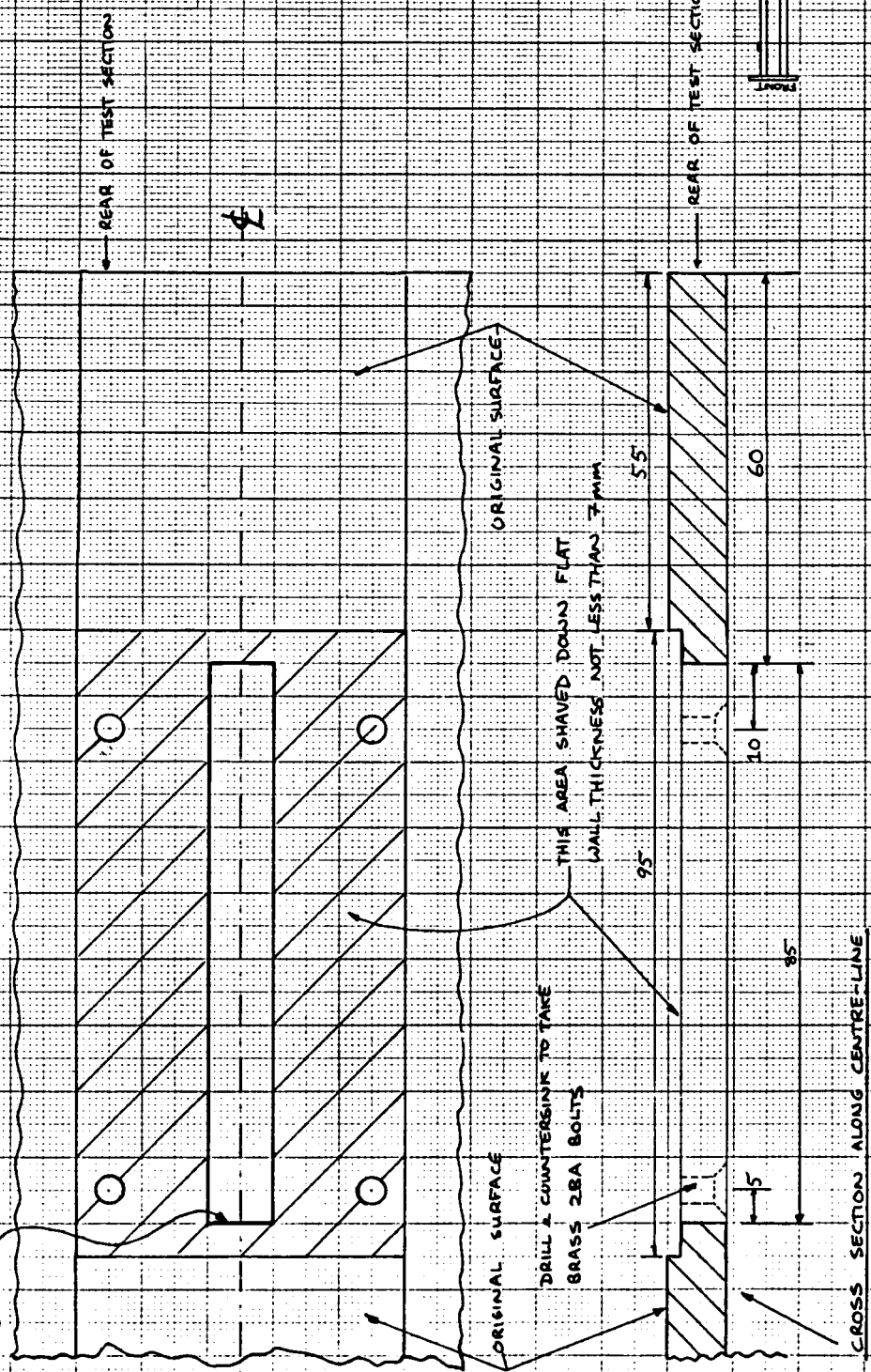


NECESSARY CHANGES TO TEST SECTION TO TAKE STING SUPPORT. ALL DIMENSIONS IN MM

Fig. 6

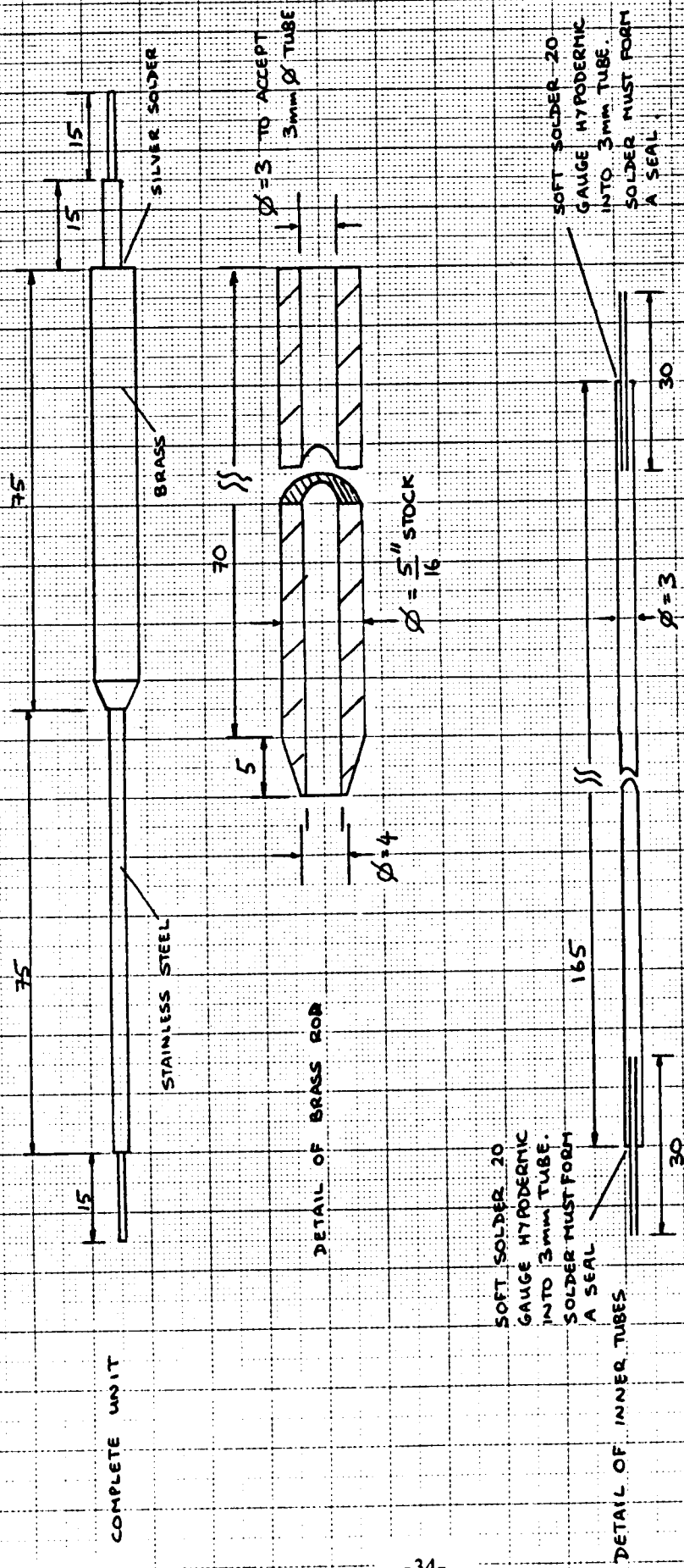
VIEW FROM ABOVE OF TOP SURFACE

STING SUPPORT BUTTS UP AGAINST THIS EDGE



ORIGINAL PAGE IS OF POOR QUALITY

Fig 8 DESIGN OF PRESSURE TAKE OFF STING DIMENSIONS IN mm UNLESS STATED OTHERWISE



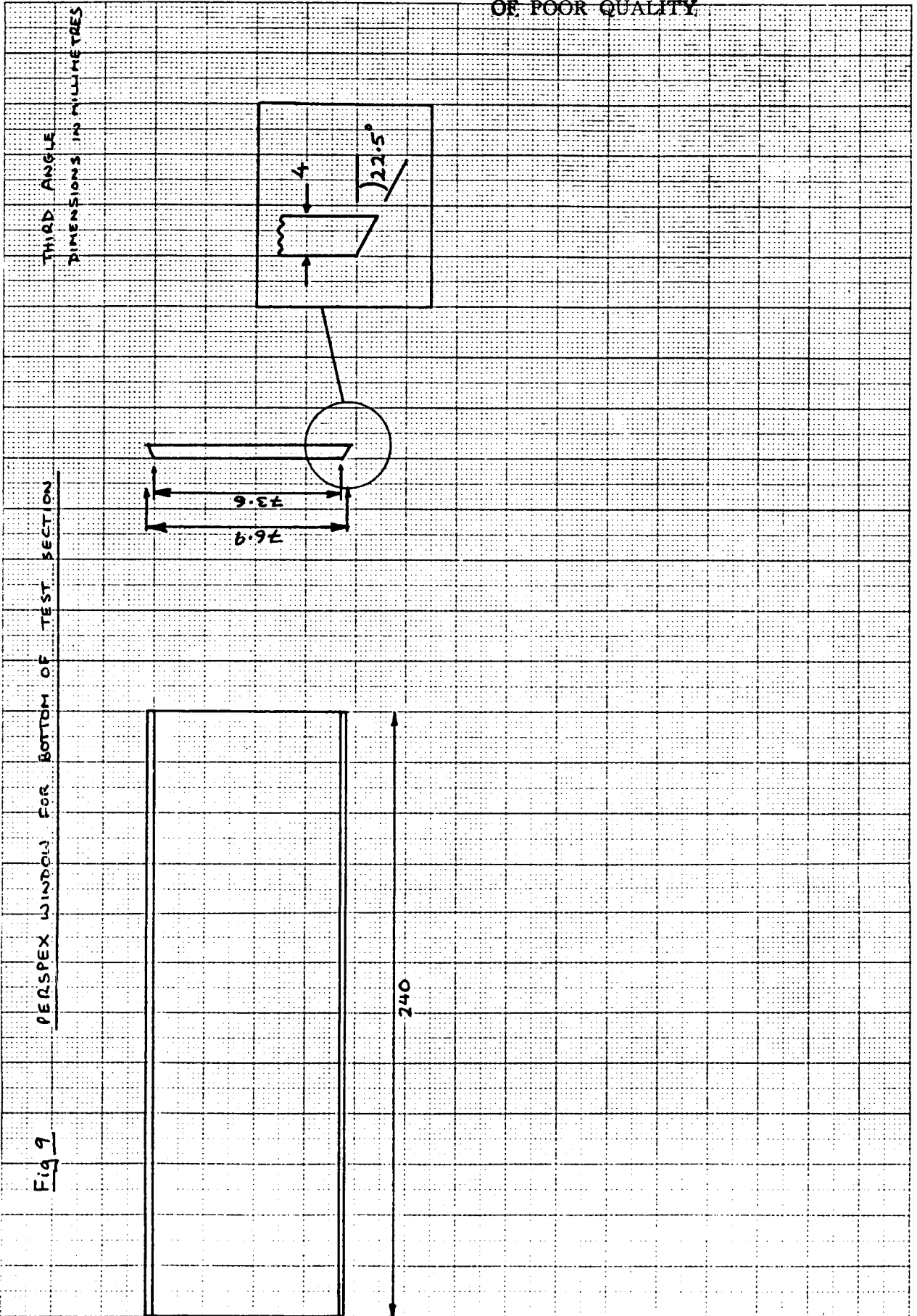
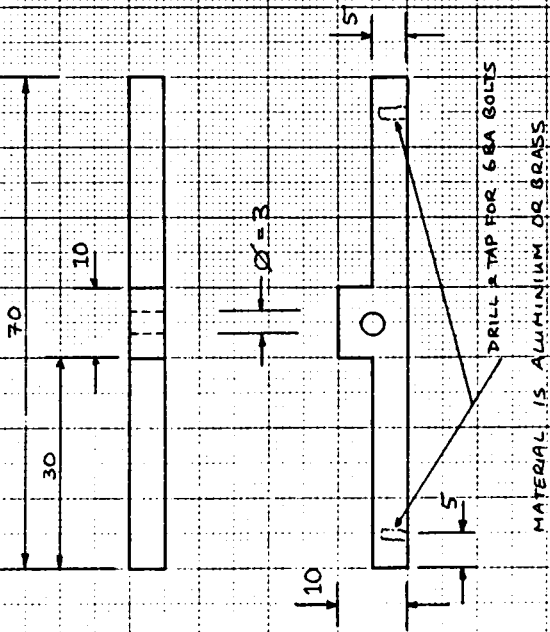


Fig 9

PERSPEX WINDOW FOR BOTTOM OF TEST SECTION

Fig 10

ROD MOUNT



ROD MOUNT & MIRROR MOUNTS

ALL DIMENSION IN MM

MIRROR MOUNTS (2OFF)

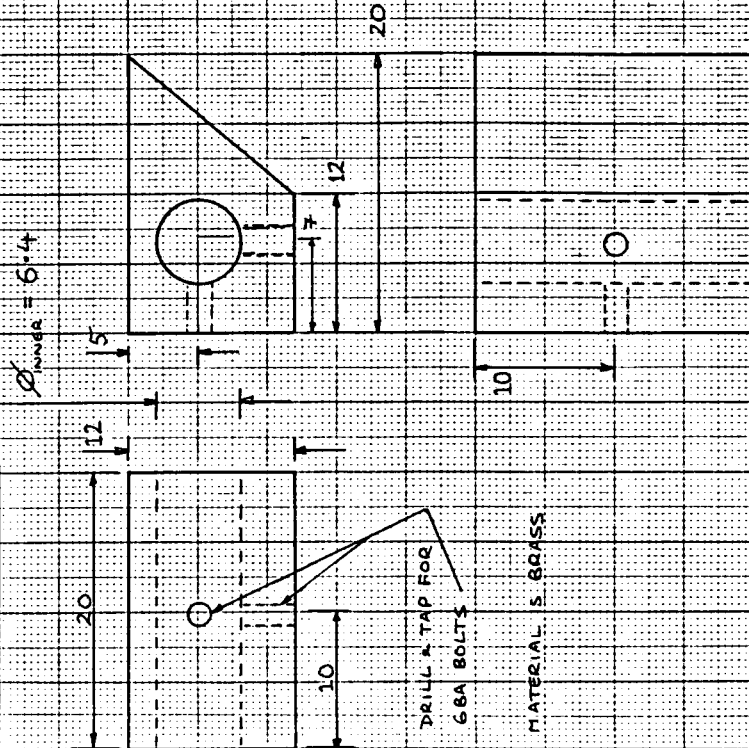


Fig 11 Dynamic Pressure Calibration

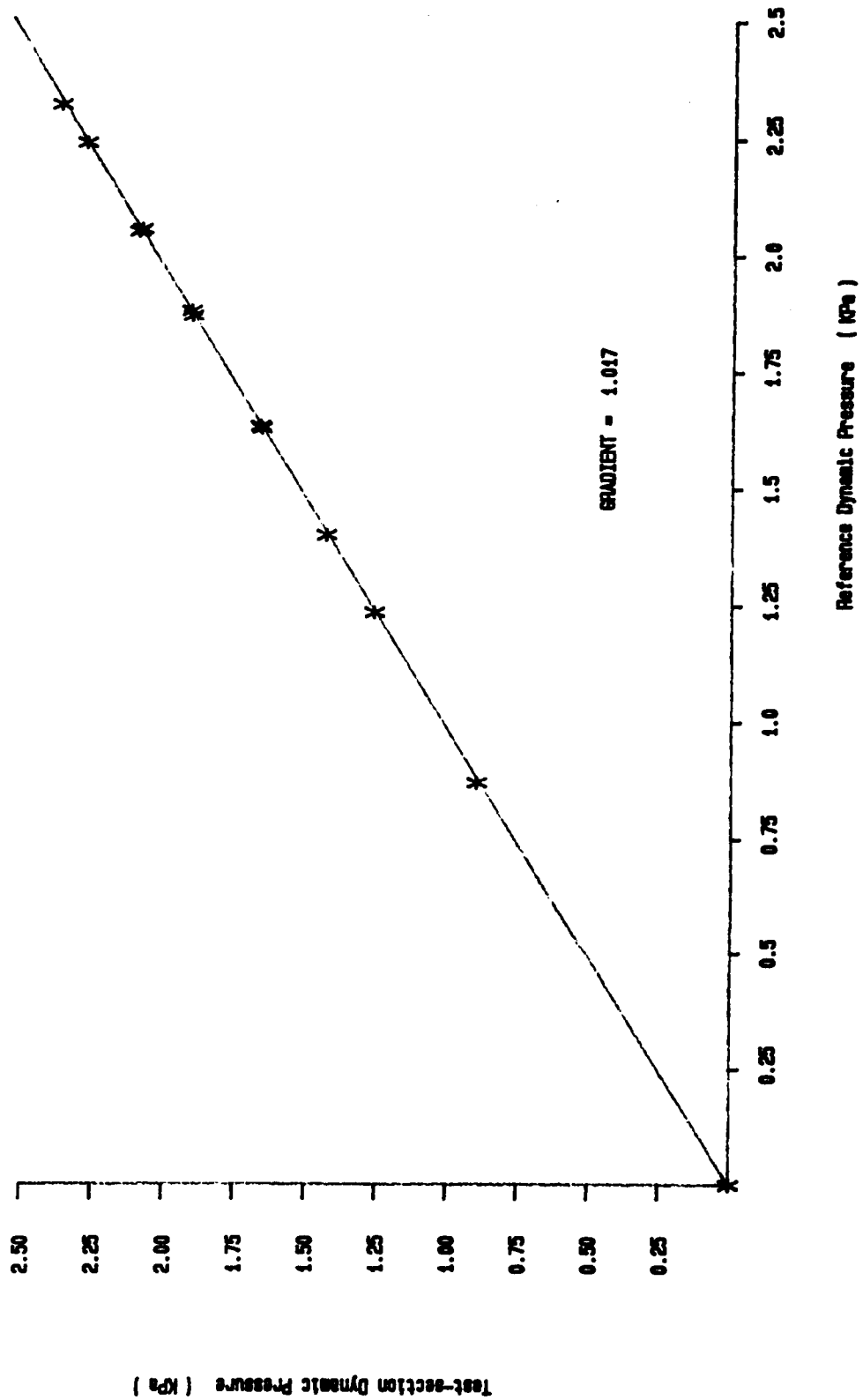


Fig 12 Axial Force-Current Calibration

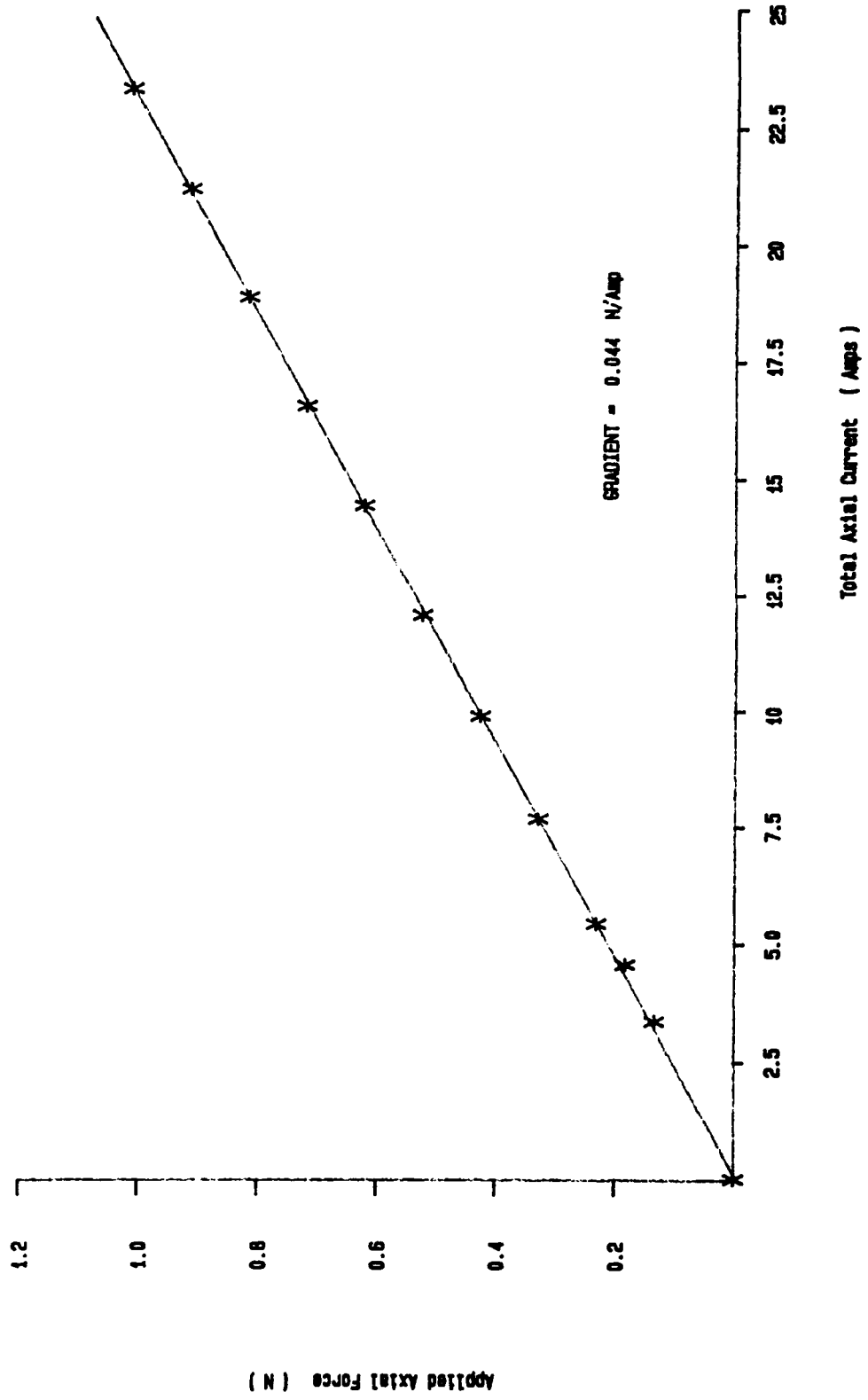
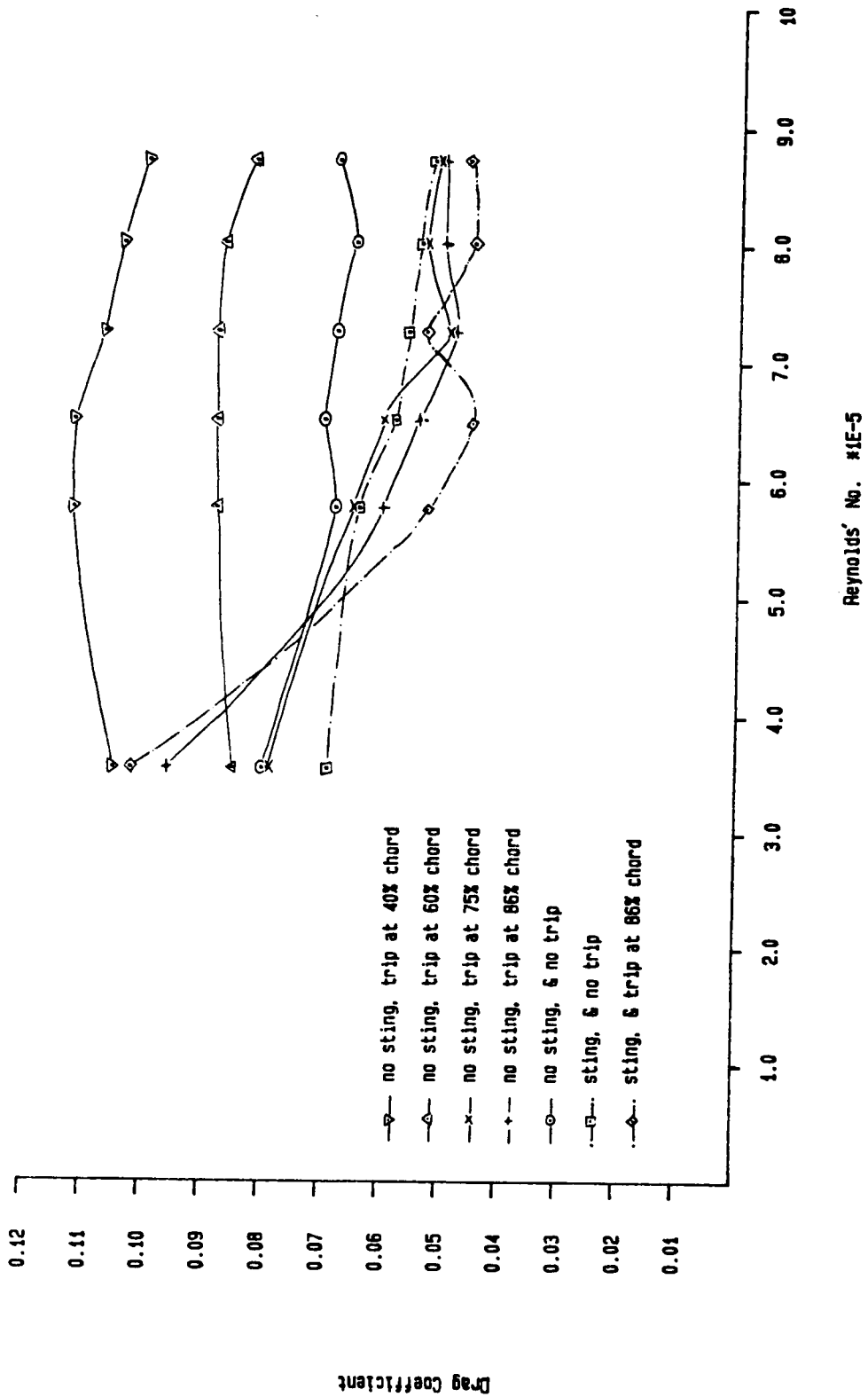


Fig 13 Drag Coefficient vs Reynolds' Number



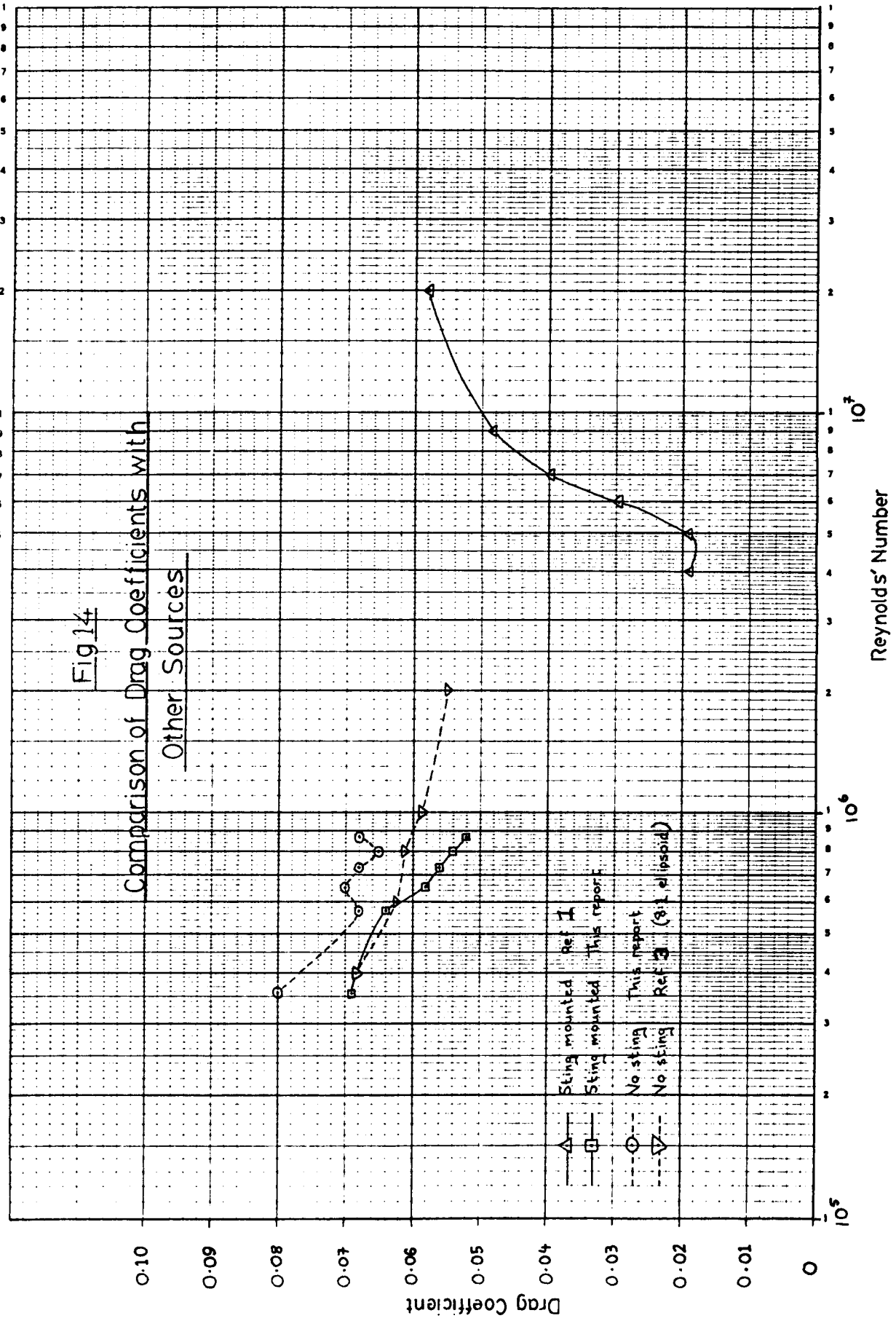


Fig 15 Variation of Cp at the two Rearmost Tappings With Reynolds' No.

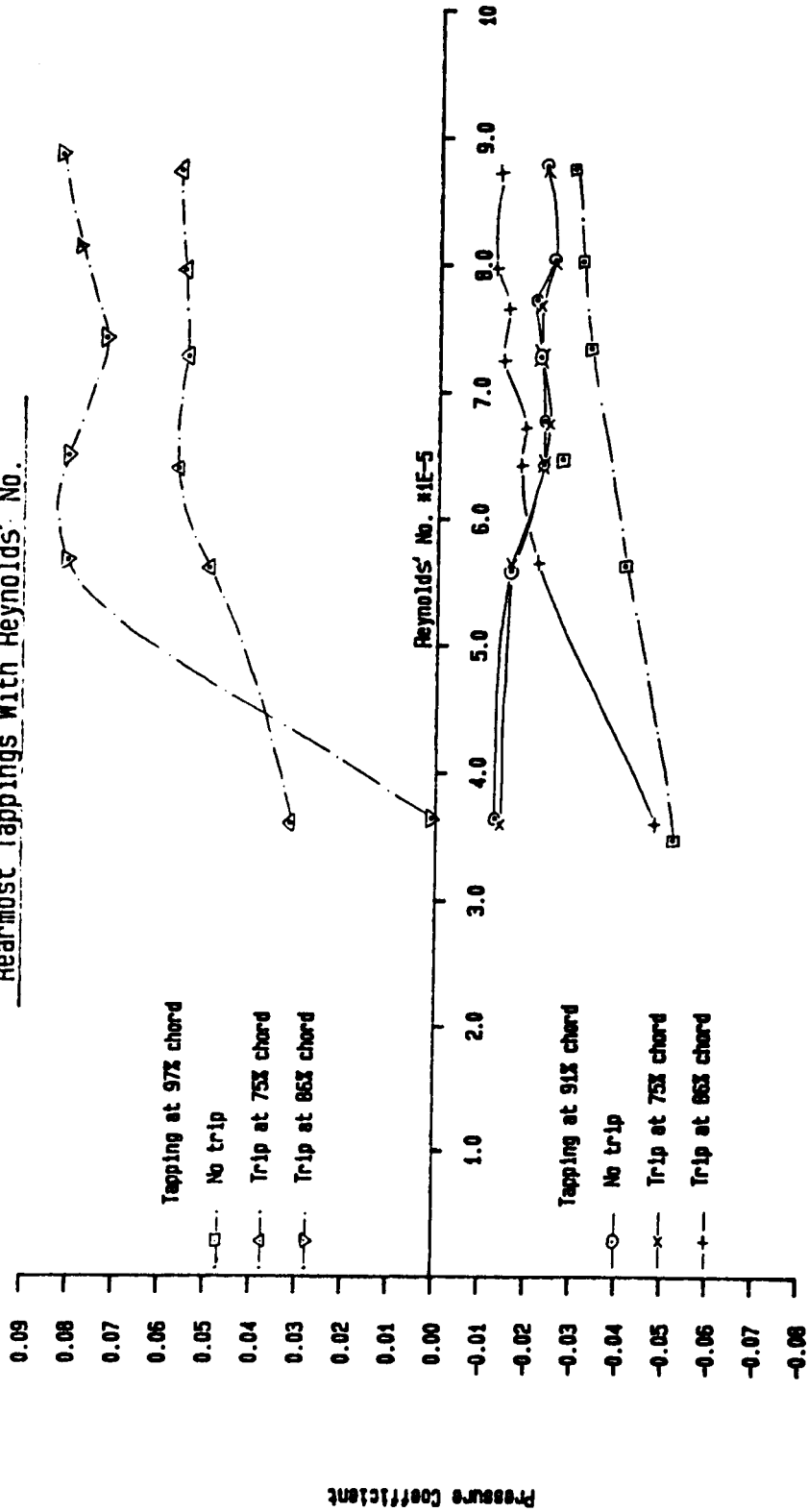


Fig 16 Variation of C_p with Axial Position

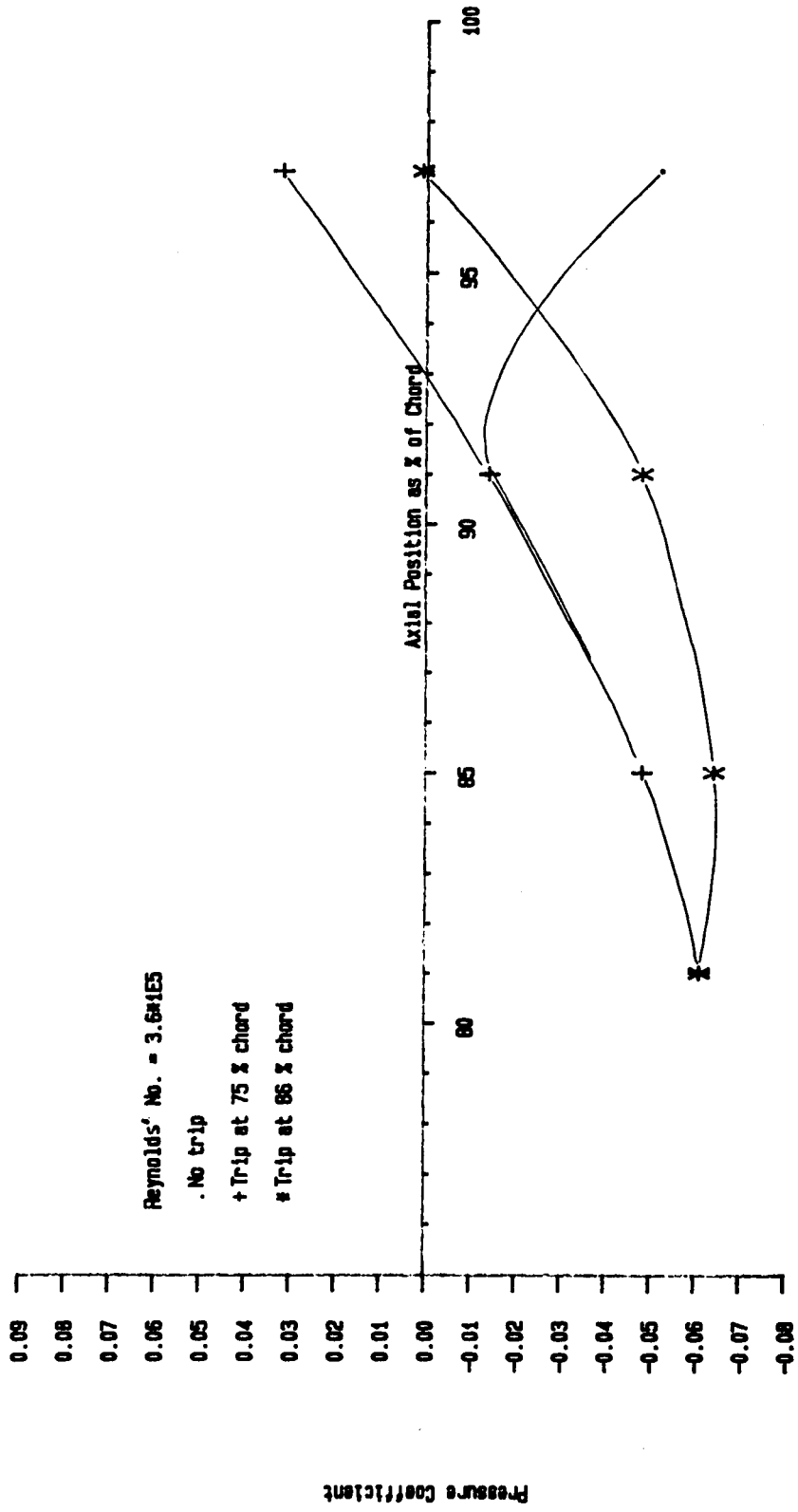


Fig 17 Variation of Cp with Axial Position

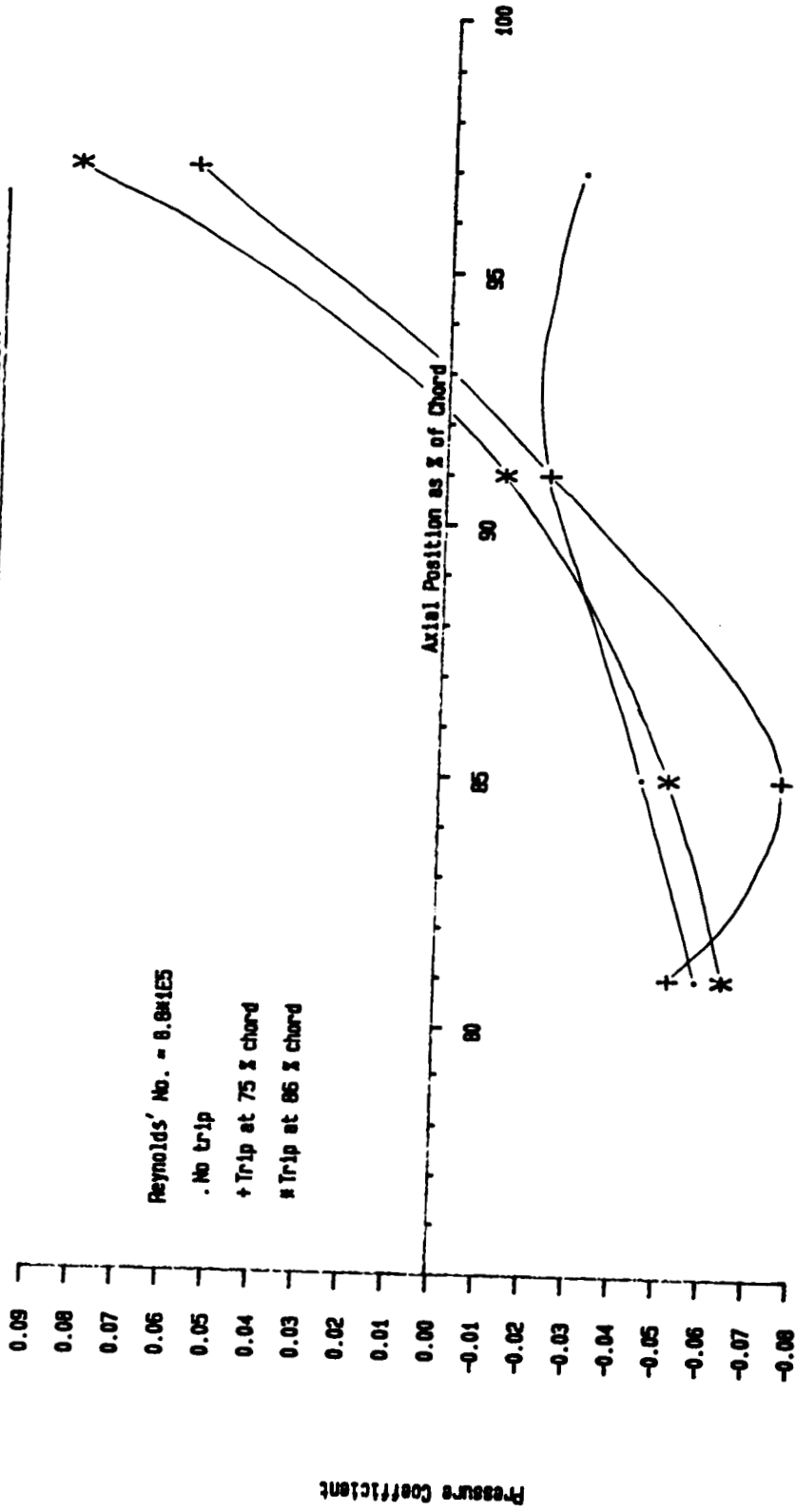


TABLE 1 : COORDINATES OF BOLTZ BODY OF REVOLUTION .in mm

X	Y	X	Y	X	Y
0	0	61.384	11.462	179.548	3.835
0.015346	0.223	64.453	11.620	181.083	3.144
0.03069	0.307	67.522	11.760	182.617	2.233
0.06138	0.449	70.592	11.882	182.771	2.199
0.09208	0.555	73.661	11.988	182.924	1.999
0.123	0.641	76.730	12.077	183.078	1.871
0.153	0.714	82.869	12.209	183.231	1.733
0.230	0.875	85.938	12.251	183.385	1.582
0.307	1.005	89.007	12.277	183.538	1.416
0.384	1.122	92.076	12.283	183.692	1.226
0.460	1.228	95.145	12.277	183.845	1.002
0.614	1.418	98.214	12.255	183.922	0.869
0.767	1.588	101.284	12.222	183.999	0.709
0.921	1.749	107.422	12.111	184.029	0.634
1.074	1.901	110.491	12.034	184.060	0.549
1.228	2.027	113.560	11.944	184.091	0.448
1.381	2.132	116.630	11.838	184.121	0.316
1.534	2.222	119.699	11.717	184.137	0.224
3.069	2.959	122.768	11.580	184.152	2.7691E-8
4.604	3.559	125.837	11.428		
6.138	4.033	128.906	11.258		
7.673	4.486	131.976	11.069		
9.210	4.862	135.045	10.863		
10.742	5.573	138.114	10.638		
13.811	5.836	141.183	10.391		
15.348	6.195	144.252	10.121		
18.415	6.758	147.322	9.826		
21.484	7.279	150.391	9.505		
24.554	7.762	153.460	9.155		
27.623	8.213	156.529	8.772		
30.692	8.633	159.598	8.351		
33.761	9.025	162.668	7.886		
33.680	9.392	165.739	7.369		
39.900	9.736	168.806	6.789		
42.370	10.055	170.341	6.470		
46.038	10.349	171.875	6.128		
49.107	10.619	173.410	5.758		
52.176	10.865	174.944	5.354		
55.246	11.086	176.480	4.909		
58.315	11.284	178.014	4.410		

ORIGINAL PAGE IS
OF POOR QUALITY.

Table 2 : Measured values of Cp and Reynolds' No. at the four static tappings

Chord 81%		85%		91%		97%	
Cp	$\frac{Re}{1E5}$	Cp	$\frac{Re}{1E5}$	Cp	$\frac{Re}{1E5}$	Cp	$\frac{Re}{1E5}$
No trip:-							
-.061	3.67	-.048	3.61	-.013	3.65	-.052	3.48
-.064	5.77	-.039	5.77	-.016	5.59	-.041	5.63
-.065	6.55	-.046	6.55	-.023	6.44	-.027	6.48
-.059	6.82	-.045	6.84	-.023	6.78	-	-
-.068	7.31	-.042	7.29	-.022	7.28	-.033	7.35
-.062	7.60	-.045	7.54	-.021	7.73	-	-
-.059	8.08	-.044	8.03	-.025	8.04	-.031	8.03
-.058	8.22	-.045	8.79	-.023	8.78	-.029	8.76
Trip at 75% chord:-							
-.061	3.67	-.048	3.61	-.014	3.60	.032	3.60
-.047	5.68	-.072	5.73	-.016	5.63	.050	5.59
-.051	6.54	-.075	6.54	-.023	6.44	.057	6.39
-.050	6.82	-.072	6.84	-.024	6.76	-	-
-.049	7.30	-.074	7.24	-.022	7.28	.055	7.27
-.048	7.61	-.076	7.61	-.022	7.69	-	-
-.044	8.04	-.076	8.03	-.025	8.02	.056	7.95
-.052	8.83	-.076	8.73	-.023	8.75	.057	8.73
Trip at 86% chord:-							
-.061	3.67	-.064	3.59	-.048	3.60	.001	3.64
-.072	5.73	-.059	5.75	-.022	5.65	.081	5.66
-.072	6.51	-.051	6.52	-.018	6.43	.081	6.49
-.069	6.79	-.059	6.79	-.019	6.73	-	-
-.070	7.23	-.053	7.30	-.014	7.25	.073	7.41
-.069	7.62	-.051	7.64	-.015	7.66	-	-
-.061	8.00	-.051	8.03	-.012	7.98	.079	8.13
-.064	8.73	-.051	8.76	-.013	8.73	.083	8.84

TABLE 3 OUTPUT FROM SPIND 1 (same data as in Table 4)

AXIAL POS ^o Count	FRONT AXIAL CURRENT (Amps)	REAR AXIAL CURRENT (Amps)	SPIN (RPM)	ROOM TEMP. (°C)	ROOM PRESSURE (RPM)	P - Pair (RPM)	P+ - Pair (RPM)	DATE
2549	-0.153	0.021	0.000	17.00	102.900	0.000	0.000	START 4116 3 H
2550	-0.252	-0.024	0.000	17.00	102.900	0.000	0.000	STOP 4116 3 H
2551	0.688	1.848	2.435	17.00	102.900	0.000	0.000	NO 4116 3 H
2549	0.782	1.993	2.435	17.00	102.900	0.000	0.000	NO 4116 3 H
2550	0.597	1.758	2.435	17.00	102.900	0.000	0.000	NO 4116 3 H
2552	0.722	1.859	2.435	17.00	102.900	0.000	0.000	NO 4116 3 H
2550	0.686	1.878	2.996	17.00	102.900	0.000	0.000	NO 4116 3 H
2548	1.136	2.296	2.996	17.00	102.900	0.000	0.000	NO 4116 3 H
2550	0.903	2.092	2.996	17.00	102.900	0.000	0.000	NO 4116 3 H
2549	0.843	2.039	2.996	17.00	102.900	0.000	0.000	NO 4116 3 H
2551	1.152	2.344	2.996	17.00	102.900	0.000	0.000	NO 4116 3 H
2550	0.869	1.991	2.996	17.00	102.900	0.000	0.000	NO 4116 3 H
2548	-0.158	-0.009	0.000	17.00	102.900	0.000	0.000	START 4116 3 I
2550	-0.249	-0.034	0.000	17.00	102.900	0.000	0.000	STOP 4116 3 I
2550	0.010	0.327	0.497	17.00	102.900	0.000	0.000	NO 4116 3 I
2552	-0.023	0.283	0.497	17.00	102.900	0.000	0.000	NO 4116 3 I
2550	-0.005	0.342	0.497	17.00	102.900	0.000	0.000	NO 4116 3 I
2549	0.021	0.406	0.497	17.00	102.900	0.000	0.000	NO 4116 3 I
2549	0.079	0.523	0.497	17.00	102.900	0.000	0.000	NO 4116 3 I
2549	0.857	2.025	2.996	17.00	102.900	0.000	0.000	NO 4116 3 I
2549	1.146	2.347	2.996	17.00	102.900	0.000	0.000	NO 4116 3 I
2549	0.970	2.154	2.996	17.00	102.900	0.000	0.000	NO 4116 3 I
2550	0.894	2.054	2.996	17.00	102.900	0.000	0.000	NO 4116 3 I
2550	0.842	2.016	2.996	17.00	102.900	0.000	0.000	NO 4116 3 I
2518	-0.175	0.005	0.000	18.00	102.900	0.000	0.000	START 5117 3 H
2545	-0.210	0.057	0.000	18.00	102.900	0.000	0.000	STOP 5117 3 H
2518	-0.113	0.390	1.987	18.00	102.900	0.350	0.415	YS 5117 3 H
2521	0.113	0.738	1.987	18.00	102.900	0.350	0.415	YS 5117 3 H
2519	-0.187	0.406	1.987	18.00	102.900	0.350	0.415	YS 5117 3 H
2522	-0.154	0.393	1.987	18.00	102.900	0.350	0.415	YS 5117 3 H
2523	-0.170	0.287	1.987	18.00	102.900	0.350	0.415	YS 5117 3 H
2518	0.061	0.486	2.483	18.00	102.900	0.464	0.472	YS 5117 3 H
2519	0.105	0.467	2.483	18.00	102.900	0.464	0.472	YS 5117 3 H
2520	0.132	0.587	2.483	18.00	102.900	0.464	0.472	YS 5117 3 H
2521	0.029	0.440	2.483	18.00	102.900	0.464	0.472	YS 5117 3 H
2522	0.048	0.385	2.483	18.00	102.900	0.464	0.472	YS 5117 3 H
2522	-0.313	-0.088	0.000	18.00	102.900	0.000	0.000	START 5117 3 I
2521	0.369	-0.106	0.000	18.00	102.900	0.000	0.000	STOP 5117 3 I
2496	0.023	0.133	0.562	18.00	102.900	-0.033	-0.041	YS 5117 3 I
2497	0.052	0.104	0.562	18.00	102.900	-0.033	-0.041	YS 5117 3 I
2491	0.049	0.311	0.562	18.00	102.900	-0.033	-0.041	YS 5117 3 I
2470	0.038	0.325	0.562	18.00	102.900	-0.033	-0.041	YS 5117 3 I
2493	0.021	0.210	0.562	18.00	102.900	-0.033	-0.041	YS 5117 3 I
2524	0.030	0.275	2.931	18.00	102.900	0.554	0.570	YS 5117 3 I
2518	0.108	0.569	2.931	18.00	102.900	0.554	0.570	YS 5117 3 I
2521	-0.018	0.388	2.931	18.00	102.900	0.554	0.570	YS 5117 3 I
2520	0.045	0.284	2.931	18.00	102.900	0.554	0.570	YS 5117 3 I
2522	0.416	0.473	2.931	18.00	102.900	0.554	0.570	YS 5117 3 I
0	0.000	0.000	0.000	0.00	0.000	0.000	0.000	... NO FILE ...

ORIGINAL PAGE IS
OF POOR QUALITY

ORIGINAL PAGE IS
OF POOR QUALITY

TABLE 4 OUTPUT FROM 490062 (same data as in Table 3)

Cd	Re	W ₀ (m.s ⁻¹)	M ₀	q ₀ (kg)	AXIAL FORCE DUE TO SUPERSONIC PRESSURES (N)	AXIAL FORCE DUE TO BASE PRESSURES (N)	DATE
0.1032	803554.	63.31	0.1854	2.476	0.12015	0.00000	ND 4T16 3 H
0.1115	803554.	63.31	0.1854	2.476	0.12975	0.00000	ND 4T16 3 H
0.0964	803554.	63.31	0.1854	2.476	0.11221	0.00000	ND 4T16 3 H
0.1049	803554.	63.31	0.1854	2.476	0.12212	0.00000	ND 4T16 3 H
0.0848	891326.	70.22	0.2057	3.047	0.12138	0.00000	ND 4T16 3 H
0.1113	891326.	70.22	0.2057	3.047	0.15744	0.00000	ND 4T16 3 H
0.0980	891326.	70.22	0.2057	3.047	0.14028	0.00000	ND 4T16 3 H
0.0945	891326.	70.22	0.2057	3.047	0.15332	0.00000	ND 4T16 3 H
0.1133	891326.	70.22	0.2057	3.047	0.16225	0.00000	ND 4T16 3 H
0.0938	891326.	70.22	0.2057	3.047	0.13436	0.00000	ND 4T16 3 H
0.1037	363031.	28.60	0.0838	0.505	0.02464	0.00000	ND 4T16 3 I
0.0895	363031.	28.60	0.0838	0.505	0.02127	0.00000	ND 4T16 3 I
0.1037	363031.	28.60	0.0838	0.505	0.02464	0.00000	ND 4T16 3 I
0.1527	363031.	28.60	0.0838	0.505	0.02859	0.00000	ND 4T16 3 I
0.0951	891326.	70.22	0.2057	3.047	0.03626	0.00000	ND 4T16 3 I
0.1138	891326.	70.22	0.2057	3.047	0.13624	0.00000	ND 4T16 3 I
0.1025	891326.	70.22	0.2057	3.047	0.16303	0.00000	ND 4T16 3 I
0.0972	891326.	70.22	0.2057	3.047	0.14685	0.00000	ND 4T16 3 I
0.0944	891326.	70.22	0.2057	3.047	0.13914	0.00000	ND 4T16 3 I
0.0420	722640.	57.29	0.1675	2.021	0.13519	0.00000	ND 4T16 3 I
0.0685	722640.	57.29	0.1675	2.021	0.01923	0.02062	YS 5T17 3 H
0.0593	722640.	57.29	0.1675	2.021	0.04440	0.02062	YS 5T17 3 H
0.0402	722640.	57.29	0.1675	2.021	0.01668	0.02062	YS 5T17 3 H
0.0346	722640.	57.29	0.1675	2.021	0.01756	0.02062	YS 5T17 3 H
0.0478	807814.	64.04	0.1872	2.525	0.01221	0.02062	YS 5T17 3 H
0.0541	807814.	64.04	0.1872	2.525	0.03107	0.02561	YS 5T17 3 H
0.0449	807814.	64.04	0.1872	2.525	0.03216	0.02561	YS 5T17 3 H
0.0645	807814.	64.04	0.1872	2.525	0.03861	0.02561	YS 5T17 3 H
0.0849	807814.	64.04	0.1872	2.525	0.02765	0.02561	YS 5T17 3 H
0.0754	384318.	30.47	0.0891	0.572	0.02607	0.02561	YS 5T17 3 H
0.0754	384318.	30.47	0.0891	0.572	0.04432	-0.00123	YS 5T17 3 I
0.0754	384318.	30.47	0.0891	0.572	0.02149	-0.00123	YS 5T17 3 I
0.0754	384318.	30.47	0.0891	0.572	0.01177	0.00173	YS 5T17 3 I
0.1046	384318.	30.47	0.0891	0.572	0.03600	-0.00123	YS 5T17 3 I
0.0652	377669.	69.58	0.2034	2.981	0.02934	0.03068	YS 5T17 3 I
0.0668	377669.	69.58	0.2034	2.981	0.03258	0.03068	YS 5T17 3 I
0.0472	377669.	69.58	0.2034	2.981	0.04889	0.03068	YS 5T17 3 I
0.0459	377669.	69.58	0.2034	2.981	0.03543	0.03068	YS 5T17 3 I
0.0540	377669.	69.58	0.2034	2.981	0.03363	0.03068	YS 5T17 3 I
0.0000	0.	0.00	0.0000	0.000	0.04503	0.03068	YS 5T17 3 I
					0.00000	0.00000	...END FILE....

APPENDIX I

CALCULATION OF PRESSURE COEFFICIENTS

The definition of pressure coefficient is

$$C_p = \frac{p_m - p_{\infty}}{q_{\infty}}$$

where

p_m is the measured pressure

p_{∞} is the free stream static pressure

q_{∞} is the free stream dynamic pressure.

The tunnel is set up so that the static pressure at the model, p_m , can be measured referenced to the reference static pressure, p_r , measured just after the contraction.

The measured difference is $p_m - p_r$

$$p_m - p_{\infty} = (p_m - p_r) - (p_{\infty} - H) + (p_r - H)$$

where H is the total pressure of the free stream.

Now, q_{∞} is related to the reference dynamic pressure, see Section 4.1, by the relationship

$$q_{\infty} = q_{REF} \cdot 1.017 = (H - p_r) \cdot 1.017$$

$$\therefore C_p = \frac{p_m - p_r}{(H - p_r) \cdot 1.017} + 1 + \frac{p_r - H}{(H - p_r) \cdot 1.017}$$

$$\therefore C_p = 1 + \frac{p_m - p_r}{(H - p_r) \cdot 1.017} - \frac{1}{1.017}$$

Hence the pressure coefficient can be calculated from the two known pressure differences $p_m - p_r$ and $H - p_r$.

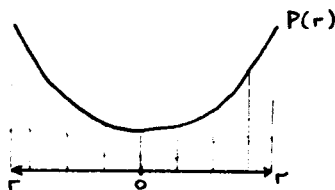
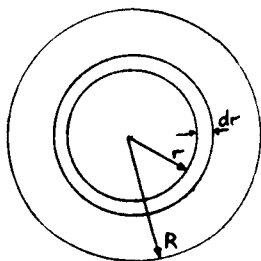
ORIGINAL PAGE IS
OF POOR QUALITY

APPENDIX II

CALCULATION OF BASEFORCE

The baseforce acting on the model with the dummy sting has to be measured. By measuring three pressures at known positions a pressure distribution is found and used to calculate the baseforce.

Assuming a quadratic pressure distribution around the centre line of the base cavity of the form $P(r) = a + br + cr^2$.



The element of area is $\delta A(r) = 2\pi r \delta r$

∴ The element of force is $\delta F(r) = P(r) \cdot \delta A(r) = 2\pi (ar + br^2 + cr^3) dr$

∴ The total baseforce is

$$F = \int_0^R 2\pi (ar + br^2 + cr^3) dr$$

$$F = 2\pi \left[\frac{ar^2}{2} + \frac{br^3}{3} + \frac{cr^4}{4} \right]_0^R$$

$$F = 2\pi \left\{ \frac{aR^2}{2} + \frac{bR^3}{3} + \frac{cR^4}{4} \right\}$$

where R is the maximum radius of the cavity.

The coefficients a, b and c are found by considering the three known pressures at the three known radii. See the listing of 4PROG2 FOR in Appendix IV.

ORIGINAL PAGE IS
OF POOR QUALITY

```

C
C PROGRAM          4PROG1.FOR
C                  A.W.NEWCOMB
C
      DIMENSION IDATA(12000),NAME(6),DATES(7)
      DIMENSION AVERS(71,8),ARRAY(50,14)
      DIMENSION IFLAG2(50),SUM(14),AV(14),AVBACH(8)
      INTEGER AXAV,H,A,F
      BYTE KEY
C
      ICOUNT=0
      IGRP=0
C
      TYPE 200
200  FORMAT(//'$ FILENAME OF DATA SOURCE -- ')
      READ(5,210)(NAME(I),I=1,6)
210  FORMAT(6A2)
      WRITE(5,805)
805  FORMAT(' RESULTING DATA TO BE STORED IN  4PROG1.STO  ')
C
      WRITE(5,822)
822  FORMAT(' INPUT ROOM TEMP CELSIUS AND PRESSURE KPA ')
      READ(5,*)RTC,RP
      OPEN(UNIT=1,NAME=NAME,TYPE='OLD',FORM='UNFORMATTED',
1RECORDSIZE=1)
      OPEN(UNIT=2,NAME='4PROG1.TEM',TYPE='SCRATCH',FORM='FORMATTED')
      OPEN(UNIT=3,NAME='4PROG1.STO',TYPE='NEW',FORM='FORMATTED')
900  CONTINUE
      AASUM=0.0
      AXSUM=0.0
      FASUM=0.0
      AAAV=0.0
      AXAV=0
      FAAV=0.0
C
876  FORMAT(' HOW MANY BLOCKS OF DATA TO BE ANALYSED --')
      WRITE(5,876)
      READ(5,877)ISETS
877  FORMAT(2I)
      NUMBER=10
      NR=NUMBER
      ND=NUMBER*16
      TYPE 101
101  FORMAT(//'$ TERMINAL(5) OR PRINTER(6) ')
      READ(5,102) IPLACE
102  FORMAT(I1)
C

```

```

953   CONTINUE
      DO 10 I=1,NR
10    READ(1) IDATA(I)
C
      XASUM=0.0
      XFSUM=0.0
      WRITE(IPLACE,20)
20    FORMAT(30X,15HCURRENTS (AMPS))
      WRITE(IPLACE,30)
30    FORMAT(3X,'LIFT',1X,'PITCH',1X,'AXIAL',4X,2HFU,4X,2HFL,4X,2HFP,
+4X,2HFS,4X,2HFA,4X,2HAU,4X,2HAL,4X,2HAP,4X,2HAS,4X,2HAA)
      DO 40 I=1,NUMBER
        J=(I-1)*16+1
        H=IDATA(J+4)+IDATA(J+1)+IDATA(J+2)+IDATA(J+3)
        P=(IDATA(J+4)+IDATA(J+3))-(IDATA(J+2)+IDATA(J+1))
        A=IDATA(J+5)
        FS=FLOAT(( *7777.AND.IDATA(J+6))-2047)*0.01221
        AS=FLOAT(( *7777.AND.IDATA(J+7))-2047)*0.01221
        FP=FLOAT(( *7777.AND.IDATA(J+8))-2047)*0.01221
        AP=FLOAT(( *7777.AND.IDATA(J+9))-2047)*0.01221
        FU=FLOAT(( *7777.AND.IDATA(J+10))-2047)*0.01221
        AL=FLOAT(( *7777.AND.IDATA(J+11))-2047)*0.01221
        FL=FLOAT(( *7777.AND.IDATA(J+12))-2047)*0.01221
        AU=FLOAT(( *7777.AND.IDATA(J+13))-2047)*0.01221
        FA=FLOAT(( *7777.AND.IDATA(J+14))-2047)*0.01221
        AA=FLOAT(( *7777.AND.IDATA(J+15))-2047)*0.01221
C
        ARRAY(I,1)=H
        ARRAY(I,2)=P
        ARRAY(I,3)=A
        ARRAY(I,4)=FU
        ARRAY(I,5)=FL
        ARRAY(I,6)=FP
        ARRAY(I,7)=FS
        ARRAY(I,8)=FA
        ARRAY(I,9)=AU
        ARRAY(I,10)=AL
        ARRAY(I,11)=AP
        ARRAY(I,12)=AS
        ARRAY(I,13)=AA
        ARRAY(I,14)=AA+FA
        XASUM=XASUM+AA
        XFSUM=XFSUM+FA
C
        IF(I.EQ.1)SIGSUMAX=0.0
        SIGSUMAX=SIGSUMAX+AA+FA
C
        TIME=FLOAT(IDATA(J))
        WRITE(IPLACE,50)(H,P,A,FU,FL,FP,FS,FA,AU,AL,AP,AS,AA)
50    FORMAT(3I6,2X,10F6.2)
        FASUM=FASUM+FA
        AASUM=AASUM+AA
        AXSUM=AXSUM+A
40    CONTINUE
        ICOUNT=ICOUNT+1
        AVERS(ICOUNT,1)=ICOUNT
        AVERS(ICOUNT,2)=XASUM/NR
        AVERS(ICOUNT,3)=XFSUM/NR
        AVERS(ICOUNT,4)=(XFSUM+XASUM)/NR

```

```

C
C *****
C ROUTINE TO CHECK FOR REJECTION
C
C -----
C CALC AVERAGE OF THE SET OF "NUMBER" READINGS
AVSUMAX=SIGSUMAX/NUMBER
C
C -----
C CALC SUM OF SQUARED DIFFERNCES FROM AVERAGE
SUMDIFFSQ=0.0
DO 700 IZ=1,NUMBER
SUMDIFFSQ=SUMDIFFSQ+(ARRAY(IZ,14)-AVSUMAX)**2
700 CONTINUE
C
C -----
C CALC STANDARD DEVIATION OF SAMPLE
STDEV1=(SUMDIFFSQ/NUMBER)**.5
WRITE(IPLACE,*) ' St dev=',STDEV1, ' average sum of
+ axial currents=',AVSUMAX
C
C -----
C CHECK FOR DATA POINT OUT OF RANGE BY USING
C CHAUVENET'S CRITERION
C THIS IS SET FOR A BLOCK OF TEN VALUES.
C IF 'NUMBER' IS CHANGED THEN CHANGE THE '1.96'
DO 710 IZ=1,NUMBER
IFLAG2(IZ)=0
IF(ARRAY(IZ,14).GE.(AVSUMAX+1.96*STDEV1))IFLAG2(IZ)=1
IF(ARRAY(IZ,14).LE.(AVSUMAX-1.96*STDEV1))IFLAG2(IZ)=1
710 CONTINUE
C
C -----
C RESET TO ZERO
DO 715 IZ=1,14
SUM(IZ)=0.0
715 CONTINUE
C
C -----
C WORK OUT NEW AVERAGES
ICNT=0
DO 720 IZ=1,NUMBER
IF(IFLAG2(IZ).EQ.1)GOTO 730
ICNT=ICNT+1
DO 740 IZ2=1,13
SUM(IZ2)=SUM(IZ2)+ARRAY(IZ,IZ2)
740 CONTINUE
SUM(14)=SUM(14)+ARRAY(IZ,8)+ARRAY(IZ,13)
730 CONTINUE
720 CONTINUE
DO 750 IZ=1,14
AV(IZ)=SUM(IZ)/ICNT
750 CONTINUE
C
C -----
C STORE AVERAGES OF FOR'D AX CUR, AFT AX CUR
C SUM OF AX CURRENTS AND AXIAL POSITION
AVERS(ICOUNT,5)=AV(8)
AVERS(ICOUNT,6)=AV(13)
AVERS(ICOUNT,7)=AV(14)
AVERS(ICOUNT,8)=AV(3)
C
C -----
C PRINT OUT 'GOOD' DATA AVERAGES
WRITE(5,*) ' Averages of "good" data... '
WRITE(IPLACE,371)(AV(JJ),JJ=1,13)
371 FORMAT(' ',3F6.0,1X,10F6.2)
WRITE(5,370)AV(14)
370 FORMAT(' Average sum of axial currents=',F5.2,' amps ')
C
C -----

```



```

C      PRINT OUT FLAGS TO SHOW WHICH DATA WAS GOOD=0,BAD=1
      WRITE(IPLACE,380)(IFLAG2(JJ),JJ=1,NUMBER)
380    FORMAT(' REJ',10(1X,2I))
      WRITE(5,*)' ..... '
C
C      HAVE THE PROPER NUMBER OF SETS BEEN ANALYSED
C      IF NOT GOTO 953
      IF(ICOUNT.NE.ISETS)GOTO 953
C
C      PRINT OUT WHICH SET AND AVERAGES
      DO 189 ICT=1,ICOUNT
      WRITE(IPLACE,360)(AVERS(ICT,JJ),JJ=1,8)
360    FORMAT(' ',7(F7.3,2X),F6.0)
189    CONTINUE
C
      DO 191 ICT=2,8
      AVBACH(ICT)=0.0
      DO 192 IZ=1,ISETS
      AVBACH(ICT)=(AVBACH(IZ)+AVERS(IZ,ICT))/ISETS)
192    CONTINUE
191    CONTINUE
      WRITE(IPLACE,360)9999.*1000.,(AVBACH(JJ),JJ=2,8)
C
C      PASS VALUES TO NEXT SECTION OF THIS PROGRAM
      AXAV=INT(AVBACH(8)+.5)
      FAAV=AVBACH(5)
      AAAV=AVBACH(6)
C
C      RESET COUNTER TO ZERO FOR NEXT BATCH OF SAMPLES
      ICOUNT=0
C      END OF REJECTION ROUTINE
C      *****
C
C      INPUT ROUTINE FOR DATE AND FLAGS
C
      WRITE(5,823)
      WRITE(5,824)
      WRITE(5,825)
      WRITE(5,826)
      WRITE(5,827)
      WRITE(5,828)
      WRITE(5,829)
      IGRP=IGRP+1
      WRITE(5,834)IGRP
834    FORMAT(' THIS IS SET NUMBER',3I)
823    FORMAT(' INPUT DATE EG 111286 ')
824    FORMAT(' IF FIRST TEST & WIND IS OFF THEN DATE="START DATE" ')
825    FORMAT(' IF LAST TEST & WIND IS OFF THEN DATE="STOP DATE" ')
826    FORMAT(' EG START 1112 OR STOP 1112 MAX 12 CHARS'
+ ,/, ' THESE ARE USED TO FIND THE ZERO WIND CURRENTS ')
827    FORMAT(' ',/, ' IF NOT START OR STOP AND ')
828    FORMAT(' ',18X,'STING OUT THEN DATE="NO DATE" EG NO 111286 ')
829    FORMAT(' ',18X,'STING IN THEN DATE="YS DATE" EG YS 111286 ')
      READ(5,833)(DATES(II),II=1,7)
833    FORMAT(7A2)
C
C      INPUT ROUTINE FOR BASE PRESSURES
C      RESET VALUES IN CASE START OR STOP RUN
      P1=0.0
      P2=0.0
      P3=0.0
C      ALSO RESET DYNAMIC PRESSURE IN CASE OF START OR STOP
      PA=0.0
C      NO NEED IF NO STING HENCE GOTO 905
      IF(DATES(1).EQ.'NO')GOTO 905

```



```

965     CONTINUE
C       READ FROM 4PROG1.STO ,WRITE TO 4CURR.TEM INCLUDE END FILE
      READ(3,840)AXAV,FAAV,AAAV,PA,RTC,RP,P1,P2,P3,(DATES(II),
+II=1,7)
      WRITE(2,840)AXAV,FAAV,AAAV,PA,RTC,RP,P1,P2,P3,(DATES(II),
+II=1,7)
      IF(DATES(1).NE.'..')GOTO 965
      GOTO 777
      WRITE(3,840)0,0.0,0.0,0.0,0.0,0.0,0.0,0.0,0.0,0.0,'..'r'EN^
+,'D ','FI','LE','..','..'
777     CONTINUE
      CLOSE(UNIT=4)
C
C       OPEN MASTER FILE AS NEW FILE THUS WIPING OUT OLD VERSION
C       & ALLOWING NEW VERSION TO BE READ IN FROM TEMP FILE
      OPEN(UNIT=4,NAME='4CURR.DAT',TYPE='NEW',FORM='FORMATTED')
      REWIND 2
967     CONTINUE
      READ(2,840)AXAV,FAAV,AAAV,PA,RTC,RP,P1,P2,P3,(DATES(II),
+II=1,7)
      WRITE(4,840)AXAV,FAAV,AAAV,PA,RTC,RP,P1,P2,P3,(DATES(II),
+II=1,7)
      IF(DATES(1).NE.'..')GOTO 967
C       CLOSE DATA FILES WIPING OUT SCRATCH FILES
      CLOSE(UNIT=4)
      WRITE(5,893)
893     FORMAT(' DATA HAS BEEN ADDED TO MASTER DATA FILE 4CURR.DAT')
970     CONTINUE
      CLOSE(UNIT=1)
      CLOSE(UNIT=2)
      CLOSE(UNIT=3)
      WRITE(5,892)
892     FORMAT(' THE DATA HAS BEEN STORED IN FILE 4PROG1.STO ')
      WRITE(5,890)
890     FORMAT(' THE LATTER FILE IS USED IN THE PROGRAM 4PROG2 ')
      END

```

```

C
C      PROGRAM          4PROG2.FOR
C                        A.W.NEWCOMB
C
C      INTEGER AXAV
C      DIMENSION DATES(7)
C      REAL LENGTH,MACH,NU
C
C      FSTART=0.0
C      FSTOP=0.0
C      ASTART=0.0
C      ASTOP=0.0
880    FORMAT(' ',4A10)
C      OPEN(UNIT=1,NAME='4PROG1.STO',TYPE='OLD',FORM='FORMATTED')
C      ***** ALL PRESSURES IN KPASCAL *****
C      ***** RELATIVE TO REFERENCE STATIC *****
C      OPEN(UNIT=2,NAME='4PROG2.STO',TYPE='NEW',FORM='FORMATTED')
900    CONTINUE
C      JJ=JJ+1
C      WRITE(5,890)JJ
890    FORMAT(' READING IN LINE....',I2)
C      READ IN DATA FROM 4PROG1.STO
C      READ(1,800)AXAV,FAAV,AAAV,PA,RTC,RP,P1,P2,P3,
+      (DATES(II),II=1,7)
800    FORMAT(I8,2X,2(F6.3,2X),F7.3,2X,F5.2,4(2X,F7.3),2X,7A2)
C      IF(DATES(1).EQ.'..'.AND.DATES(7).EQ.'..')GOTO 910
C
C      IF(DATES(1).NE.'ST'.OR.(DATES(2).NE.'AR'.AND.DATES(2).NE.'OP'))
+GOTO 945
C      WRITE(5,880)'CURRENT ', 'OFFSETS ', 'RESET'
C      IF(DATES(2).EQ.'OP')GOTO 946
C      FSTART=FAAV
C      ASTART=AAAV
C      GOTO 944
946    CONTINUE
C      FSTOP=FAAV
C      ASTOP=AAAV
944    CONTINUE
C      NO NEED TO CALCULATE VALUES AS CURRENT RESET RUN THROUGH
C      GOTO 900
945    CONTINUE
C      CONVERT CURRENTS TO FORCES
C      CURROFFSET=.5*(FSTART+ASTART+FSTOP+ASTOP)
C      FORCEFACTOR=0.04385
C      AXFORCE=FORCEFACTOR*(FAAV+AAAV-CURROFFSET)

```

```

C
      IF(PA.NE.FB)GOTO 940
      WRITE(5,804)
      WRITE(5,805)
804   FORMAT(' DYNAMIC PRESSURE=0.0 , RUN WILL CONTINUE ')
805   FORMAT(' DATA WILL BE STORED AS OVERFLOWS          ')
C     MAKE NUMBERS TOO LARGE FOR FORMATTED OUTPUT
C     OR SET TO 0.0
      CD=999.0
      REY=0.0
      V=0.0
      MACH=0.0
      PDYNTRUE=0.0
      GOTO 960
940   CONTINUE
C
C     *****
C     CALC TRUE TEST SECTION DYNAMIC PRESSURE
      DYNFACTOR=1.017
      PDYNTRUE=PA*DYNFACTOR
      IF(PA.GE.0.0)GOTO 930
      WRITE(5,850)
850   FORMAT(' DYNAMIC PRESSURE < 0.0 WILL TAKE MODULUS ')
      PDYNTRUE=PDYNTRUE*-1
930   CONTINUE
C
C     *****
C     CALC ROOM DENSITY
      RHO=RP/(287*(RTC+273.15))*1000
C
C     *****
C     CALC NU
      RECMUD=56085.3
      NU=((RTC+273.15)/288.16)**.8/RHO/RECMUD
C
C     *****
C     CALC BASE FORCE
C     IS STING IN PLACE?
C     IF NOT GOTO 905
      BASEFORCE=0.0
      IF(DATES(1).NE.'YS')GOTO 905
C     STING IS IN HENCE PROCEED
C           .....ASSUMING QUADRATIC DISTRIBUTION
C           .....OF PRESSURES OVER THE BASE AREA.
C           .....HAVE RADII IN MILLIMETRES
C           .....TO MAKE NUMBERS BETTER

```



```

C
C      OPEN DRAG FILE AS A NEW FILE. THIS WIPES OUT THE OLD DATA
C      & ALLOWS OLD & NEW DATA TO BE READ IN FROM TEMP FILE
C      OPEN(UNIT=4,NAME='4CDRAG.DAT',TYPE='NEW',FORM='FORMATTED')
      REWIND 3
967    CONTINUE
      READ(3,810)CD,REY,V,MACH,PDYNTRUE,AXFORCE,BASEFORCE,
+(DATES(II),II=1,7)
      WRITE(4,810)CD,REY,V,MACH,PDYNTRUE,AXFORCE,BASEFORCE,
+(DATES(II),II=1,7)
      IF(DATES(1).NE.'..')GOTO 967
C      CLOSE DATA FILES WIPING OUT THE SCRATCH FILE ON 3
      CLOSE(UNIT=3)
      CLOSE(UNIT=4)
      WRITE(5,839)
839    FORMAT(' NEW DATA HAS BEEN ADDED ONTO DRAG FILE 4CDRAG.DAT ')
970    CONTINUE
      CLOSE(UNIT=1)
      CLOSE(UNIT=2)
C
      WRITE(5,840)
840    FORMAT(' NEW DATA HAS BEEN STORED SEPARATELY IN 4PROG2.STO ')
      END

```



```

; .TITLE CONTR ;DECLARE PROGRAM TITLE
;
; .GLOBL CONTR,KEYBD,CHARS,COMMAN ;GLOBAL SYMBOLS
;
; .MCALL TRANSL,ROTATE,PHASEF,OUTPUT ;AND REQUIRED MACROS
; .MCALL ADCOL,INTEG,START,TRANS2,ADST ;
; .MCALL ADCOLS,TIME,DAST,ROLL ;
; .MCALL .EXIT
;
; GAIN BLOCK
;
HG: .WORD 19000. ;HEAVE GAIN
PG: .WORD 22000. ;PITCH
SG: .WORD 19000. ;SLIP
YG: .WORD 26000. ;YAW
AG: .WORD 17000. ;AXIAL
RG: .WORD 4. ;ROLL
;
; DEFINE HARDWARE ADDRESSES
;
CLBS=170432 ;CLOCK (B) STATUS
OUT=167774 ;DIGITAL OUTPUT BUFFER
ADISR=167770
ADBR=ADSR+2
; CALL STARTUP ROUTINE
;
CONTR: START OSCILL,COMMAN,CHARS,DATA ;CALL START MACRO
;
;SET-UP FOR TSX
;
MOV #LOKJOB,R0 ;LOCK JOB IN MEMORY
EMT 375
;
MOV #PRI,R0 ;SET-UP PRIORITY
EMT 375
;
MOV #SETSG,R0 ;SET-UP SINGLE CHARACTER MODE
EMT 375
;
MOV #SETNW,R0 ;SET-UP NO WAIT MODE
EMT 375
;
MOV #SETI,R0
EMT 375
;
-----
; INITIALISE CHARS STORE WITH VALUES DEFINED AT BOTTOM
;
MOV @#FACTOR,CHARS+26. ;INITIALISE CHARS+26.
MOV @#STMAIN,CHARS+40. ;
MOV @#STREF,CHARS+50. ;
MOV #0.,CHARS+52. ;
MOV @#THRESH,CHARS+54. ;
;

```

```

;
;*****
; MAIN LOOP START, CALL KEYBOARD HANDLING ROUTINE
START: JSR    PC,KEYBD           ;CALLS KEYBD SUBROUTINE
        TST    CHARS           ;ARE WE FINISHED ? (ESC)
        BEQ    SYNCHR         ;JUMP IF NOT
        RTS    PC              ;RETURN TO FORTRAN IF YES
;
; LOOP SYNCHRONISATION
;
SYNCHR: INC    CHARS+138.        ;INCREMENT MASTER COUNTER
        BIC    #176000,CHARS+138. ;REDUCE COUNTER TO 10 BITS
CLOCK: TSTB   @#CLBS           ;IS CLOCK DONE COUNTING(TO OVERFLOW)
        BPL    CLOCK          ;WAIT IF NO
        BICB   #200,@#CLBS     ;CLEAR CLOCK DONE BIT
        MOV    #151777,@#OUT    ;SETS CHANNEL 14 D/A TO -2.5V APPROX.
;
; CHANGE R6 TO DATA STACK
;
        MOV    SP,STACK        ;ARCHIVE SYSTEM STACK POINTER
        MOV    DATA,SP       ;SET UP DATA STACK
;
        TIME                ;STORE TIME                <1>
;
;*****
; RESET SOME VALUES?
TST    CHARS+12.             ;CHECK CHARS+12 [ ? ]
BEQ    AWN3                  ;IF=0 BRANCH TO AWN3
;
MOV    CHARS+26.,FACTOR     ;RESET FACTOR [ F ]
MOV    CHARS+40.,STMAIN     ;RESET STMAIN [ M ]
MOV    CHARS+50.,STREF      ;RESET STREF [ R ]
TST    CHARS+52.           ;= 0.0? [ S ]
BEQ    AWN4                 ;IF = 0.0 GOTO AWN4
MOV    RF,STREF             ;RESET STREF WITH RF
AWN4:  MOV    #0.,CHARS+52.   ;RESET TO 0.0
        MOV    CHARS+54.,THRESH ;RESET THRESHOLD[ T ]
        MOV    #0.,CHARS+12.   ;RESET FLAG [ ? ]
AWN3:  ; BRANCHED TO HERE
;
-----
; EXTRA ROUTINE TO ALTER AX READING OF MAIN DRAG
; SENSOR TO COUNTERACT DRIFT.
        MOV    STREF,RO       ;LOAD RO WITH INITIAL VALUE
        SUB    RF,RO          ;SUB SENSOR FROM INITIAL
;
CMP    RO,THRESH
BGT    AWN1                  ;DIFF>THRESH
NEG    THRESH                ;THRESH=-THRESH
CMP    RO,THRESH
NEG    THRESH                ;RESET THRESH TO +VE VALUE
BLT    AWN1                  ;DIFF<-THRESH
JMP    AWN2                  ;-THRESH<= DIFF >=+THRESH
;
AWN1:  AC1=X1
        AC2=X2
        LDCIF  RO,AC1        ;AC1=RO=DIFF
        MULF   #FACTOR,AC1   ;AC1=FACTOR*DIFF
        DIVF   #TSD,AC1      ;AC1=FACTOR*DIFF/1000
        LDCIF  AX,AC2        ;AC2=MAIN DRAG SENSOR VALUE
        SUBF   AC1,AC2       ;AC2=MAIN-FACTOR*DIFF/1000
        STCFI  AC2,AX        ;STORE AC2 AS AXIAL
AWN2:  ; JUMP HERE IF NO CHANGE NEEDED
;
-----

```

;STORE POSITION SENSOR INFO

```
MOV    FP,R0
DAST   R0           ;STORE FP           <2>
MOV    FS,R0
DAST   R0           ;STORE FS           <3>
MOV    AP,R0
DAST   R0           ;STORE AP           <4>
MOV    AS,R0
DAST   R0           ;STORE AS           <5>
MOV    AX,R0
DAST   R0           ;STORE AX           <6>
```

;
;
;
;
;

;
; COMPUTE MODEL POSITION AND ATTITUDE
; AND COLLECT SOME CURRENT DATA

```
ADST   8.           ;INITIATE FRONT ST/BD A/D
```

;
;

```
MOV    FP,R1       ;FETCH MAIN POSITION SENSOR SIGNALS
MOV    FS,R2       ;FP=FORWARD PORT,AS=AFT STARBOARD; ETC.
MOV    AP,R3       ;
MOV    AS,R4       ;
```

;HEAVE

```
MOV    R1,R0       ;LOAD R0 WITH FP
ADD    R2,R0       ;ADD ALL FOR HEAVE
ADD    R3,R0       ;
ADD    R4,R0       ;
SUB    #27777,R0   ;REMOVE HEAVE OFFSET (27777)*****
MOV    R0,HEAVE    ;STORE HEAVE POSITION
ADCOLS ;COLLECT FRONT ST/BD           <7>
ADST   10.         ;INITIALISE AFT STARBOARD
```

;PITCH

```
MOV    R4,R0       ;LOAD R0 WITH AS
ADD    R3,R0       ;ADD OTHER AFT
MOV    R1,R5       ;LOAD R5 WITH FP
ADD    R2,R5       ;ADD FS TO FP
SUB    R5,R0       ;CALC PITCH
MOV    R0,PITCH    ;STORE PITCH ATTITUDE
ADCOLS ;COLLECT AFT STARBOARD         <8>
ADST   11.         ;INITIALISE FRONT PORT
```

;SLIP

```
MOV    R1,R0       ;LOAD R0 WITH FP
ADD    R3,R0       ;ADD OTHER PORT
SUB    R2,R0       ;SUBTRACT STARBOARDS
SUB    R4,R0       ;
MOV    R0,SLIP     ;STORE SLIP POSITION
```

;YAW

```
MOV    R1,R0       ;LOAD R0 WITH FP
SUB    R2,R0       ;SUBTRACT OTHER FRONT
ADD    R4,R0       ;ADD AS
SUB    R3,R0       ;SUBTRACT OTHER AFT
MOV    R0,YAW      ;STORE YAW ATTITUDE
ADCOLS ;COLLECT FRONT PORT           <9>
ADST   13.         ;INITIATE AFT PORT
```

;AXIAL

```
MOV    AX,R0       ;LOAD R0 WITH AX
SUB    STMAIN,R0   ;REMOVE AXIAL OFFSET
ASH    #3,R0       ;AXIAL SENSITIVITY BY 4
NEG    R0          ;CORRECT SIGN
MOV    R0,AXIAL    ;STORE AXIAL POSITION
```

```

;
; LOOP RATE INDICATOR FLIP
;
      MOV      #151777,@#OUT      ;SETS CHANNEL 14 I/A TO -2.5V APPROX.
;
;*****
; COMPENSATOR WITH INTERLEAVED DATA AQUISITION
;
;INITIATE DATA AQUISITION
      ADCOLS      ;COLLECT AFT PORT          <10>
      ADST      15.      ;FORWARD UPPER CURRENT A/D START
;
;HEAVE
      PHASEF     HEAVE,HT,0.44,8.0,2.5      ;PHASE ADVANCE HEAVE POSITION
      TRANSL     CHARS,OSCILL,6             ;ADD IN USER DEMANDS
      INTEG      CHARS,HINT,14.,HG         ;INTEGRATOR
      MUL        R3,R2                      ;HEAVE GAIN. DROP LOW ORDER PRODUCT
      MOV        R2,H0                      ;STORE HEAVE DEMAND
;
;COLLECT DATA AND INITIATE NEXT
      ADCOLS      ;COLLECT FU CURRENT          <11>
      ADST      12.      ;AFT LOWER CURRENT
;
;PITCH
      PHASEF     PITCH,PT,0.37,6.0,3.1      ;PHASE ADVANCE PITCH ATTITUDE
      ROTATE     CHARS,OSCILL,4             ;ADD IN USER DEMANDS
      INTEG      CHARS,PINT,30.,PG         ;INTEGRATOR
      MUL        R3,R2                      ;PITCH GAIN
      MOV        R2,PO                      ;STORE PITCH DEMAND
;
;COLLECT DATA AND INITIATE NEXT
      ADCOLS      ;COLLECT AL CURRENT          <12>
      ADST      9.      ;FORWARD LOWER CURRENT
;
;SLIP
      PHASEF     SLIP,ST,0.44,8.0,2.5      ;PHASE ADVANCE SLIP POSITION
      TRANSL     CHARS,OSCILL,4             ;ADD IN USER DEMANDS
      INTEG      CHARS,SINT,36.,SG         ;INTEGRATOR
      MUL        R3,R2                      ;SLIP GAIN
      MOV        R2,SO                      ;STORE SLIP DEMAND
;
;COLLECT DATA AND INITIATE NEXT
      ADCOLS      ;COLLECT FL CURRENT          <13>
      ADST      7.      ;AFT UPPER CURRENT
;
;YAW
      PHASEF     YAW,YT,0.37,6.0,3.1      ;PHASE ADVANCE YAW ATTITUDE
      ROTATE     CHARS,OSCILL,6             ;ADD IN USER DEMANDS
      INTEG      CHARS,YINT,48.,YG         ;INTEGRATOR
      MUL        R3,R2                      ;YAW GAIN
      MOV        R2,YO                      ;STORE YAW DEMAND
;
;COLLECT DATA AND INITIATE NEXT
      ADCOLS      ;COLLECT AU CURRENT          <14>
      ADST      14.      ;FORWARD AXIAL CURRENT
;
;AXIAL
      PHASEF     AXIAL,AT,0.54,12.0,1.6    ;PHASE ADVANCE AXIAL POSITION
      TRANS2     CHARS,2                    ;ADD IN USER DEMANDS
      INTEG      CHARS,AINT,0.,AG         ;INTEGRATOR
      MUL        R3,R2                      ;AXIAL GAIN
      MOV        R2,AO                      ;STORE AXIAL DEMAND
;
;COLLECT DATA AND INITIATE NEXT
      ADCOLS      ;COLLECT FA CURRENT          <15>
;
;
      ADST      6.      ;AFT AXIAL CURRENT
;

```

```

;
;
;MODEL OUT DETECTOR
;
OUTON:  CMP      #6777,HEAVE      ;TEST HEAVE POSITION
        BPL      MODIN           ;JUMP TO OUTPUTS IF MODEL IS IN
; MODEL OUT
        CLR      HO              ;CLEAR ALL FINAL DEMANDS
        CLR      PO              ;IF MODEL IS OUT
        CLR      SO
        CLR      YO
        CLR      AO
        CLR      HINT            ;INCLUDING HIGH ORDER
        CLR      PINT            ;INTEGRATOR ACCUMULATORS
        CLR      SINT
        CLR      YINT
        CLR      AINT
;
MODIN:
;
;COLLECT DATA
        ADCOLS                    ;COLLECT AA CURRENT          <16>
;
;*****
;OUTPUT ROUTINES WITH INTERLEAVED POSITION SENSOR DATA COLLECTION
;INITIATE A/D
;FRONT STAR/BD
        ADST      5.              ;START FS A/D
;
;
;FORWARD UPPER OUTPUT
        MOV      HO,R0            ;FETCH HEAVE DEMAND
        SUB      PO,R0            ;SUBTRACT PITCH DEMAND
        OUTPUT   10000           ;CALL OUTPUT ROUTINE
;FORWARD LOWER OUTPUT
        MOV      PO,R0            ;FETCH PITCH DEMAND
        SUB      HO,R0            ;SUBTRACT HEAVE DEMAND
        OUTPUT   70000           ;CALL OUTPUT ROUTINE
;
        ADCOL     FS              ;COLLECT
;AFT STAR/BD
        ADST      3.              ;INITIATE AS A/D
;
;AFT UPPER OUTPUT
        CLR      R0              ;SET R0 TO ZERO
        SUB      HO,R0            ;SUBTRACT HEAVE DEMAND
        SUB      PO,R0            ;SUBTRACT PITCH DEMAND
        OUTPUT   110000          ;CALL OUTPUT ROUTINE
;AFT LOWER OUTPUT
        MOV      HO,R0            ;FETCH HEAVE DEMAND
        ADD      PO,R0            ;ADD PITCH DEMAND
        OUTPUT   40000
;
        ADCOL     AS              ;COLLECT
;FRONT PORT
        ADST      4.              ;INITIATE FP A/D
;
;FORWARD PORT OUTPUT
        MOV      SO,R0
        ADD      YO,R0
        OUTPUT   50000
;FORWARD STARBOARD OUTPUT
        CLR      R0
        SUB      SO,R0
        SUB      YO,R0
        OUTPUT   100000

```

```

;
; ADCOL FP ;COLLECT
;AFT PORT
ADST 2. ;INITIATE AP A/D
;
;AFT PORT OUTPUT
MOV YO,R0 ;FETCH YAW DEMAND
SUB SO,R0 ;SUBTRACT SLIP DEMAND
OUTPUT 30000 ;CALL OUTPUT ROUTINE
;AFT STARBOARD OUTPUT
MOV SO,R0 ;FETCH SLIP DEMAND
SUB YO,R0 ;SUBTRACT YAW DEMAND
OUTPUT 60000 ;CALL OUTPUT ROUTINE
;
; ADCOL AP ;COLLECT
;AXIAL
ADST 0. ;INITIATE AXIAL A/D
;
;AFT AXIAL OUTPUT
MOV AO,R0 ;FETCH AXIAL DEMAND
OUTPUT 20000 ;CALL OUTPUT ROUTINE
MOV AO,R0 ;FETCH AXIAL DEMAND
OUTPUT 120000 ;CALL OUTPUT ROUTINE
;
; ADCOL AX ;COLLECT AXIAL A/D
;
; ADST 1. ;INITIATE REFERENCE SENSOR
; A/D CONVERSION
;
; DBGB: MOV #4,R0
; DEC R0 ; ----DELAY-----
; TST R0
; BPL DBGB
;
; ADCOL RF ;COLLECT SENSOR DATA
;
; DELAY FOR OUTPUT PORT TO PERFORM JOB BEFORE LOOP RATE FLOP
; JMP DBG7
; DELAY REMOVED
; DBG7:
;
; LOOP RATE INDICATOR FLOP
;
; MOV #155777,@#OUT ;SETS CHANNEL 14 D/A TO +2.5V APPROX.
;
; *****
; PRESERVE DATA ?
; TST CHARS+132. ;IS ( SET +VE (STORE) ?
; BEQ NOSAMP ;JUMP OUT IF NO
; DEC CHARS+132. ;KEEP DATA AND REDUCE CYCLE COUNTER
; BR JUMPST ;DONE HERE
; NOSAMP: SUB #32.,SP ;DISCARD DATA
;
; RESTORE SYSTEM STACKS, RETURN TO LOOP START
;
; JUMPST: MOV SP,DATA ;ARCHIVE DATA STACK POINTER
; MOV STACK,SP ;RESTORE SYSTEM STACK
; JMP START ;BACK TO ;START
;
; *****
; DECLARE VARIABLES
;
; CHARS: .BLKW 72. ;STORAGE OF INPUT COMMAND DATA
; DATA: .WORD 0,0 ;ADDRESSES OF DATA ARRAY
; STACK: .WORD 0 ;SYSTEM STACK POINTER
; OSCILL: .WORD 0 ;ADDRESS OF OSCILLATOR ARRAY

```

```

;
HEAVE: .WORD 0 ;MODEL HEAVE POSITION
SLIP: .WORD 0 ;SLIP POSITION
AXIAL: .WORD 0 ;AXIAL POSITION
PITCH: .WORD 0 ;PITCH ATTITUDE
YAW: .WORD 0 ;YAW ATTITUDE
;
FP: .WORD 0 ;FORWARD PORT POSITION SENSOR
FS: .WORD 0 ;FORWARD STARBOARD
AP: .WORD 0 ;AFT PORT
AS: .WORD 0 ;AFT STARBOARD
AX: .WORD 0 ;AXIAL
RF: .WORD 0 ;AXIAL REFERENCE SENSOR
;
FACTOR: .WORD 0. ;SCALAR
THRESH: .WORD 0. ;INITIAL THRESHOLD FOR
;REFERENCE SENSOR
;
TSD: .WORD 1000. ;TSD=1000.
STREF: .WORD 2849. ;INITIAL REFERENCE SENSOR VALUE
STMAIN: .WORD 2630. ;INITIAL MAIN AXIAL SENSOR VALUE
;
;
HO: .WORD 0 ;FINAL HEAVE DEMAND
PO: .WORD 0 ;PITCH DEMAND
SO: .WORD 0 ;SIDE DEMAND
YO: .WORD 0 ;YAW DEMAND
AO: .WORD 0 ;AXIAL DEMAND
;
HT: .FLT2 0.,0. ;INTERMEDIATE DATA STORAGE
PT: .FLT2 0.,0. ;FOR PHASE ADVANCERS
ST: .FLT2 0.,0. ;
YT: .FLT2 0.,0. ;
AT: .FLT2 0.,0. ;
;
HINT: .WORD 0,0 ;INTEGRATOR ACCUMULATORS
PINT: .WORD 0,0 ;(HIGH AND LOW WORDS)
SINT: .WORD 0,0 ;
YINT: .WORD 0,0 ;
AINT: .WORD 0,0 ;
;
;TSX+ EMT BLOCKS
;
LOKJOB: .BYTE 13,140
PRI: .BYTE 0,150
.WORD 127.
;
SETSG: .BYTE 0,152
.WORD 'S
SETNW: .BYTE 0,152
.WORD 'U
SETI: .BYTE 0,152
.WORD 'I
;
.END

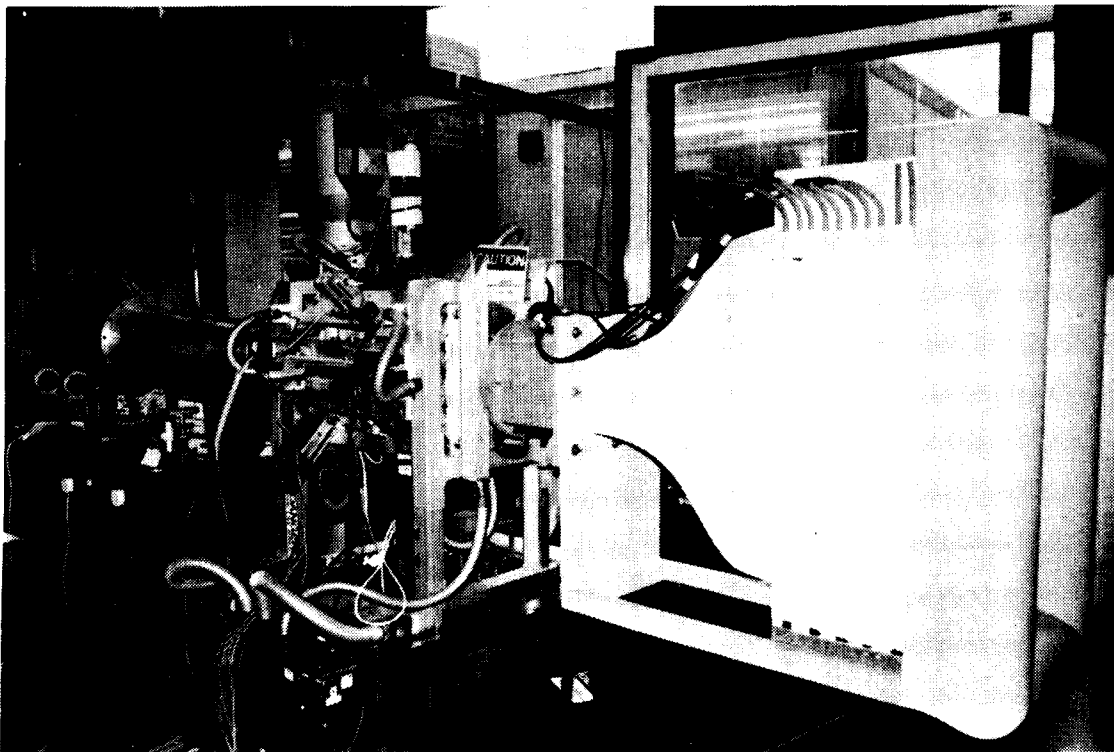
```

THIS VERSION TO BE USED FOR DRAG TESTING WITHOUT STING
OR TESTING WITH STING IF MODEL IS FORWARD OF THE STING.

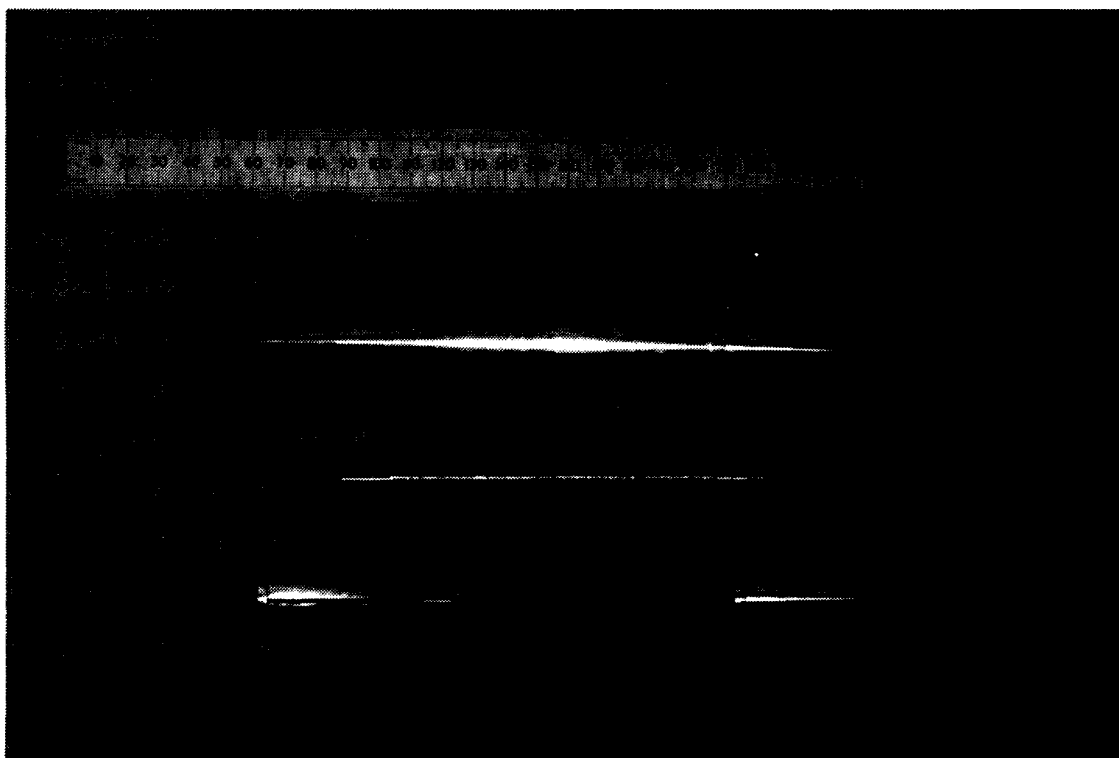
```
50      1  h  make sure the intesrators are on
400     10  f  take data
87      10  f
87      10  f
87      10  f
87      10  f
0       0  0  the end ****
```

THIS VERSION TO BE USED IF STING IS INSIDE BASE CAVITY
OR FOR PRESSURE DISTRIBUTION INVESTIGATION.

```
50      1  h  make sure the intesrators are on
400     10  f  take data
87      10  f
87      10  f
87      10  f
87      10  f
0       0  0  the end ****
```

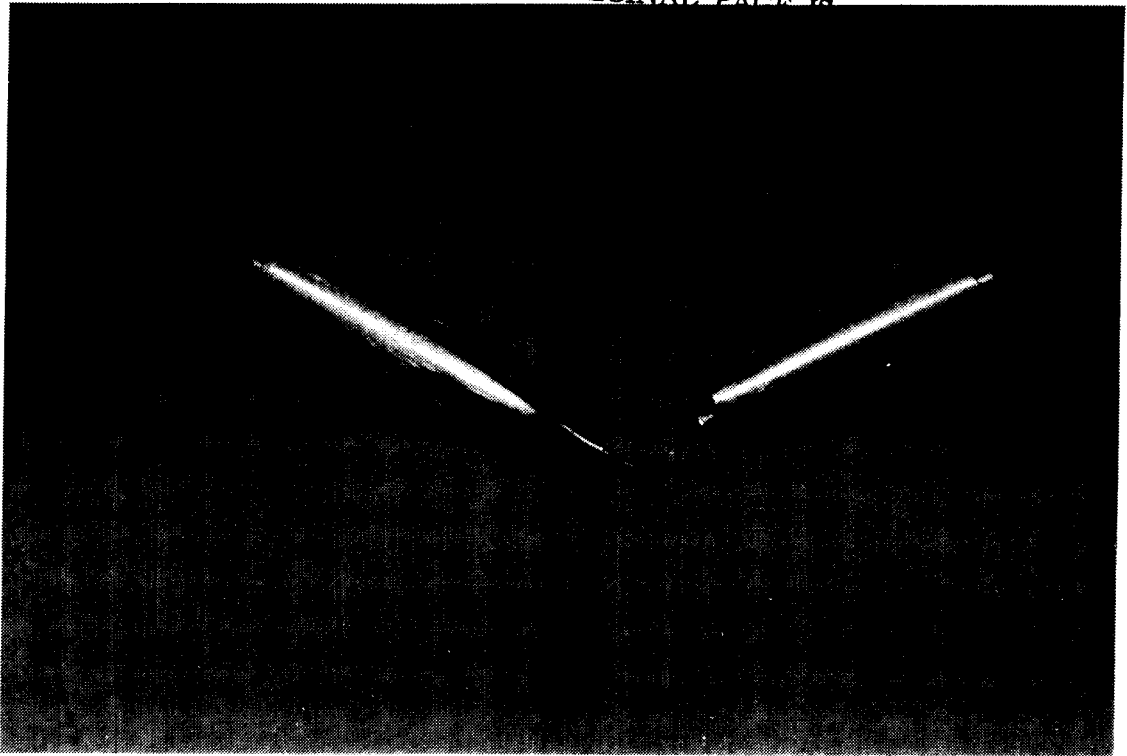



THE LOW SPEED WIND TUNNEL

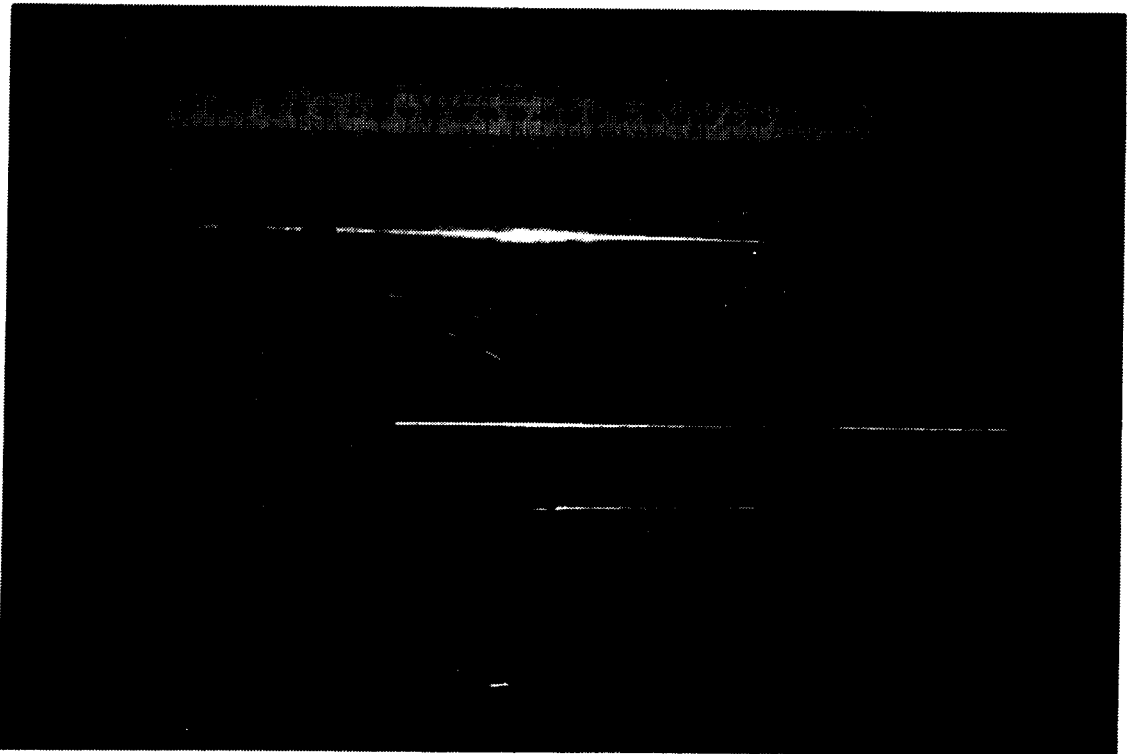


THE BOLTZ BODY, SAMARIUM COBALT MAGNETIC CORE, THE PRESSURE MEASURING REAR BODY, THE DUMMY STING BODY

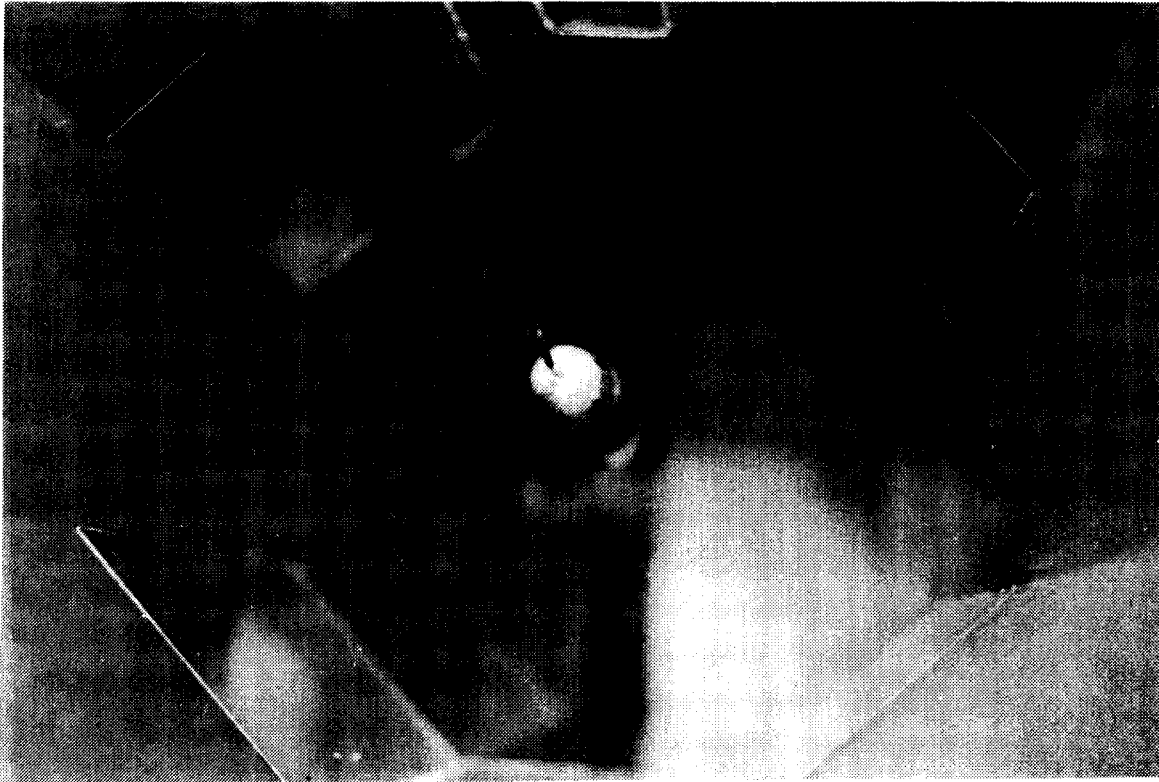
ORIGINAL PAGE IS
OF POOR QUALITY



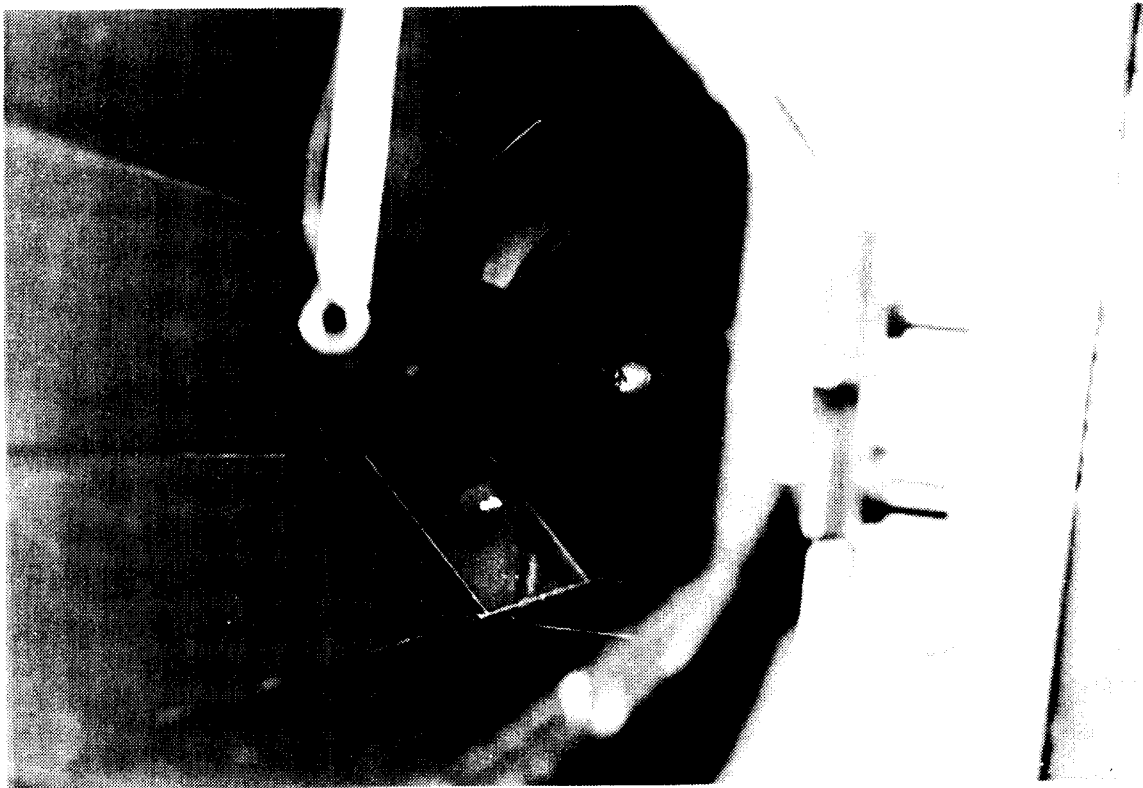
CLOSE UP OF PRESSURE DISTRIBUTION MEASURING REAR BODY AND DUMMY STING
REAR BODY



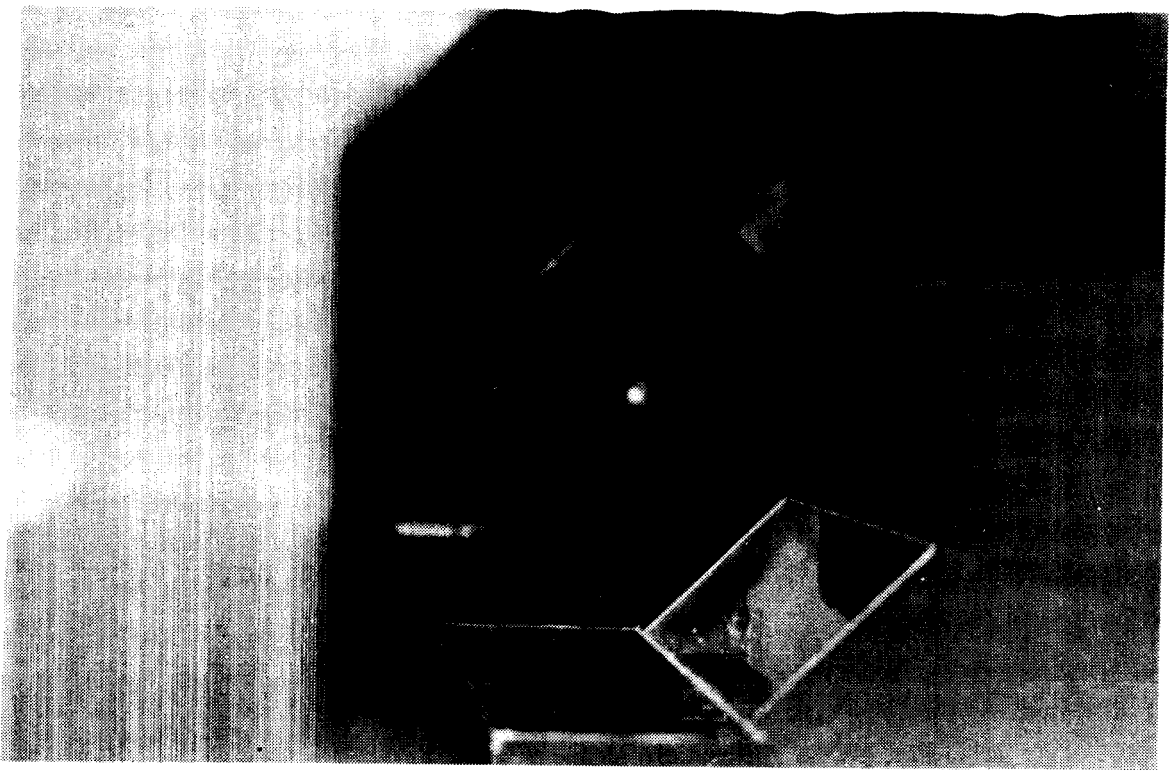
TOP TO BOTTOM: THE STING SUPPORT SLEEVE, THE DUMMY STING, AND THE
PRESSURE DISTRIBUTION MEASURING STING



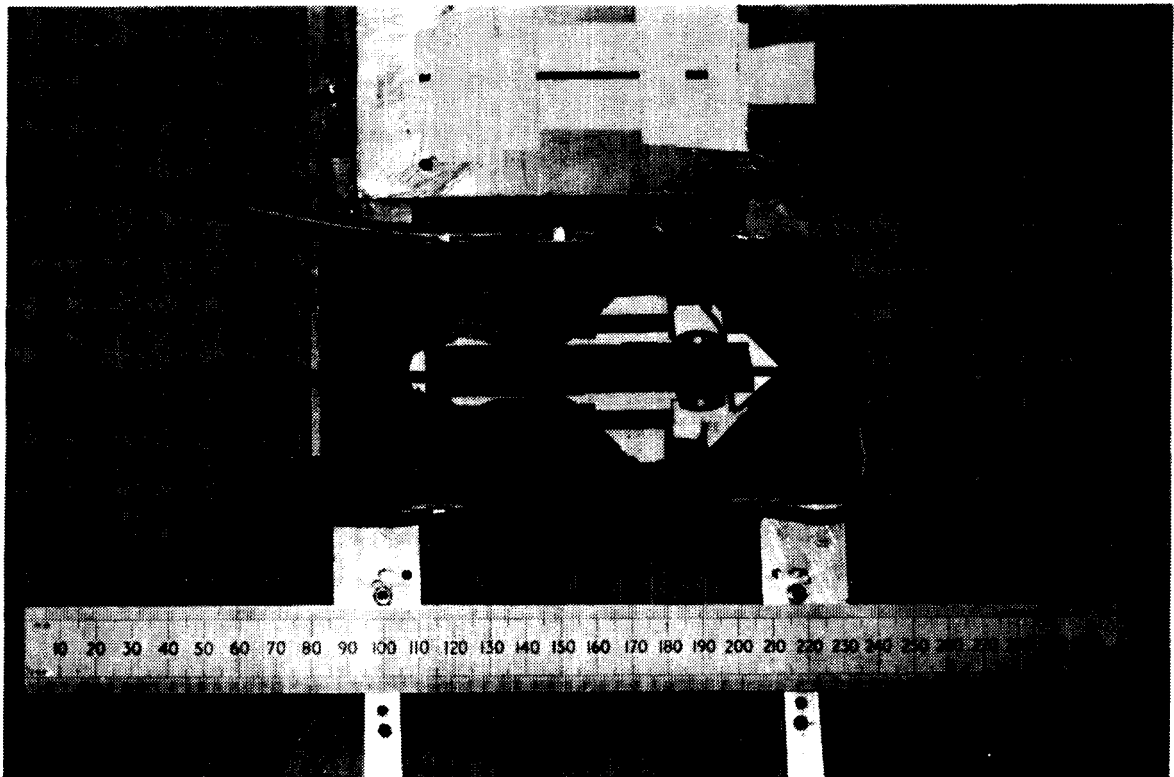
THE PRESSURE DISTRIBUTION MODEL IN SUSPENSION (VIEWED FROM REAR)



THE PRESSURE DISTRIBUTION MODEL IN SUSPENSION, NOTE THE STING SUPPORT
STRUT AND SLEEVE (VIEWED FROM REAR)



THE PRESSURE DISTRIBUTION MODEL IN SUSPENSION (VIEWED FROM FRONT)



THE AXIAL POSITION DETECTOR, NOTE THE LARGE WINDOW FOR THE MAIN DETECTOR
AND SMALLER WINDOW FOR THE REFERENCE DETECTOR



Report Documentation Page

1. Report No. NASA CR-181611		2. Government Accession No.		3. Recipient's Catalog No.	
4. Title and Subtitle The Effect of Sting Interference at Low Speeds on the Drag Coefficient of an Ellipsoidal Body Using a Magnetic Suspension and Balance System				5. Report Date February 1988	
				6. Performing Organization Code	
7. Author(s) A. W. Newcomb				8. Performing Organization Report No.	
				10. Work Unit No. 505-61-01-02	
9. Performing Organization Name and Address Vigyan Research Associates, Inc. 28 Research Road Hampton, VA 23666				11. Contract or Grant No. NAS1-17919	
				13. Type of Report and Period Covered Contractor Report	
12. Sponsoring Agency Name and Address National Aeronautics and Space Administration Washington, DC 20546				14. Sponsoring Agency Code	
15. Supplementary Notes NASA Langley Research Center Technical Monitor: Charles L. Ladson Principal Investigator: Dr. M. J. Goodyer					
16. Abstract <p>A Boltz body of revolution (finessness ratio 7.5:1) was tested in the SUMSBS. The effects of sting interference on the drag coefficient of the model at zero angle of attack were noted as well as the effects on drag coefficient values of boundary layer trips. The drag coefficient values were compared with other sources and seemed to show agreement.</p> <p>The pressure distribution over the rear of the model with no sting interference was investigated including the use of boundary layer trips.</p>					
17. Key Words (Suggested by Author(s)) Magnetic Suspension and Balance System Sting Interference Body of Revolution			18. Distribution Statement Unclassified - Unlimited Subject Category - 02		
19. Security Classif. (of this report) Unclassified		20. Security Classif. (of this page) Unclassified		21. No. of pages 79	22. Price A05